Materials Advances

ROYAL SOCIETY OF CHEMISTRY

REVIEW

View Article Online
View Journal | View Issue

Cite this: *Mater. Adv.*, 2022, 3, 3784

MXene wearables: properties, fabrication strategies, sensing mechanism and applications

Vaishakh Kedambaimoole, [ab] Kajol Harsh, [b] Konandur Rajanna, [a] Prosenjit Sen, [b] M. M. Nayak[b] and Saurabh Kumar *[bc]

Received 10th December 2021,
Accepted 14th March 2022

DOI: 10.1039/d1ma01170g

rsc.li/materials-advances

The current pandemic has forced the healthcare system into a transformation where the patients are required to be continuously monitored without the need for hospitalization. The advances in wearable sensors with their ability to sense various body parameters precisely have helped in accelerating the personalized healthcare revolution. The selection of sensing material and its properties lay the foundation for designing flexible sensors and carrying out reliable measurements. Sensing materials for wearable applications, in general, are expected to be flexible, biocompatible, electrically conducting, electrochemically active, and of low cost. Ti_3C_2–MXene is a new two-dimensional transition metal carbide that belongs to the family of MXenes, which meets many of the material requirements for biochemical sensing applications. In the present work, we discuss the properties of Ti_3C_2–MXene in detail and analyze its potential in the development of wearable biosensors. A review of recent developments in this rapidly developing field and suggestions for future research directions are presented.

1. Introduction

The world healthcare system is going through a transformation in which personalized healthcare, point-of-care diagnostics, remote patient monitoring, and healthcare internet-of-things are rapidly evolving. Wearable devices have recently seen a surge in both research and commercialization.[1,2] However, the development of commercial-grade wearable sensors has seen both progress and setbacks. The latest advances in nanotechnology, miniaturization, wireless sensing technologies, embedded

[a] *Dept of Instrumentation and Applied Physics, Indian Institute of Science, Bangalore 560012, India*
[b] *Center for Nano Science and Engineering (CeNSE), Indian Institute of Science, Bangalore 560012, India*
[c] *Department of Medical Devices, National Institute of Pharmaceutical Education and Research Guwahati, Assam, 781101, India.*
E-mail: saurabh@niperguwahati.in, sau2203@gmail.com

Vaishakh Kedambaimoole

Vaishakh Kedambaimoole received his Master of Science and PhD in engineering from Indian Institute of Science Bangalore. He is currently working as a postdoctoral researcher at the University of Cambridge. His research mainly focuses on 2D materials and their applications in flexible electronics.

Saurabh Kumar

Saurabh Kumar is currently an Assistant Professor at the Medical Devices Department at the National Institute of Pharmaceutical Education and Research (NIPER)-Guwahati, India. He received his PhD (2017) from Delhi Technological University, India. Next, Saurabh worked as a postdoctoral fellow at the material science and engineering division, KAUST, Jeddah, till July 2018. After that, he joined as an INSPIRE Faculty fellow (Aug 2018 – July 2021) at the Centre for Nanoscience and Engineering (CeNSE), Indian Institute of Science, Bangalore, India. His research focuses on biosensors, flexible and wearable sensors, 2D nanomaterials, and medical devices.

systems, and flexible electronics make it possible to develop smart systems that continuously provide personalized health monitoring.[3,4] Soft wearable sensors are devices that can be worn onto the human skin in accordance with the body architecture to continuously and closely monitor health. In this context, epidermal electronic systems are developed at the laboratory stage for clinically diagnosing respiration rate, heart rate, skin temperature, electromyography, and perspiration rate.[5–9] While biocompatible and biodegradable electronics in the form of soft wearable and implantable devices could clinically monitor a person's health, they can also serve as tools for the treatment of diverse diseases.[10] Similarly, multiple research groups have developed wearable devices for monitoring real-time data of various electrolytes and metabolites non-invasively using textile and tattoo-based sensors that perform accurately *in situ* measurements.[11] However, most wearables still rely on decade-old sensing techniques. For example, transdermal glucose monitors depend on enzyme electrodes in the form of low-cost finger prick test strips.[12] In fact, the transdermal glucose sensing device is arguably the only widespread wearable sensor that quantitatively measures the glucose concentration in blood and monitors the status of the underlying disease. The potential diagnostic capabilities of epidermal sensors can be realized by addressing key technological challenges in manufacturing and establishing reliable correlation to standard sensing modalities.[10]

Two-dimensional (2D) materials are promising candidates as active sensor materials due to their excellent physical and chemical properties. Their large surface area, ease of surface functionalization leading to enhanced chemical and electrochemical activity, optical sensitivity, and mechanical strength all mean that these materials are promising for biosensing applications. In recent years, a new class of two-dimensional materials known as MXenes has emerged as a promising prospect for wearable applications. MXenes are layered 2D materials made of transition metal carbides, nitrides, or carbonitrides. MXene is synthesized by selective etching of the parent material called the MAX phase. MAX is a layered metal carbide/nitride or carbonitride structure with the general formula $M_{X+1}AX_n$ (n = 1, 2, 3). Here M is a transition metal, A stands for the element of group 13 and 14, and X is carbon and/or nitrogen. The A layer is chemically and selectively etched that results in an $M_{X+1}X_n$ structure known as MXene. During the synthesis, the MXene layer is terminated by surface moieties such as oxygen, hydrogen, and fluorine. Hence, MXenes are presented as $M_{X+1}X_nT_x$, where T_x represents the surface functional group. A few notable examples of MXene include Ti_2CT_x, $Ti_3C_2T_x$, and $Nb_4C_3T_x$. Since the discovery of $Ti_3C_2T_x$, the first MXene to be synthesized, various compositions have been subsequently produced and dozens more are theoretically predicted to exist.[13] $Ti_3C_2T_x$ is the most explored and widely used MXene, known for its 2D nature, metallic conductivity, and hydrophilicity. Its atomically thin nature paves the way for a distinct set of properties including anisotropic electron transport behavior, excellent electrochemical properties, and flexibility. The large surface area, excellent piezoresistive behavior, and solution processibility make $Ti_3C_2T_x$ a promising material for wearable sensing applications.

The prevailing mood of the science community towards MXene research has encouraged many researchers to review and outline the recent advances in this domain. Several articles have been published detailing the aspects of MXene based sensors and wearables.[14–20] While these articles made efforts to cover all strands from materials to applications, the vastness of MXene wearables forced them to revolve around specific sections. As it is impossible to cover every detail under single review, we have contributed our part by addressing a few aspects which were not covered in detail in earlier papers. The current review highlights the recent advances in MXene-based wearable biomedical sensors. The focus was set on the use of $Ti_3C_2T_x$, one of the most widely explored MXenes to date in developing flexible and body mountable devices. A comprehensive study on the material properties, sensor fabrication aspects, and design criteria is carried out. Further, the practicable applications towards health monitoring and their existing limitations are elaborated. Finally, we conclude this review with an outline of research aspects that would impart significant advances towards the future of MXene wearables.

2. MXene chemistry in wearable sensors

2.1 Electrical conductivity

Materials that can react to external stimuli *via* a change in their electrical conductivity are highly popular in the realm of wearable sensing. To exhibit such sensing behavior, the sensing material should possess good electrical conductivity. The discovery of MXenes has opened up new prospects in wearable sensing as most MXenes are predicted to have metallic conductivity, while a few combinations exhibit semiconductor behavior. The surface functional groups are strongly coupled to the electronic properties of MXene. The high electronegativity of oxygen and fluorine groups imparts higher work functions, while hydroxyl functionalization renders an ultra-low work function, due to the strong surface dipole moment.[21] Interestingly, a band can be formed on some transition metals just by changing the surface functional groups. Consequently, the functional groups can offset the density states at the Fermi level thereby affecting the electronic conductivity and band structure. For example, any surface termination on d1 transition metals (Sc and Y) exhibits semiconducting behavior, whereas d2 transition metals in contrast (Ti, Zr, and Hf) require oxygen termination to initiate the bandgap. Moreover, the structural defects and mixed surface groups introduced during the synthesis of MXene influence its electrical conductivity. In addition to that, the etching process and intercalation method can also have an impact on the conductivity of MXene as intercalation of the Li+ cation results in better conductivity than organic intercalation,[22] as shown in Table 1. The flake size can also potentially affect the electronic transport in MXene films. The high electrical conductivity of MXene with controlled alignment of 2D sheets enables the piezoresistive sensing mechanism suitable for wearable sensing applications.

Table 1 Conductivity of different MXenes that are synthesized using various etching and intercalation techniques and comparison with the conductivity of other 2D materials

Materials	Synthesis method	Conductivity (S cm^{-1})	Ref.
Mo_2C–MXene	HF etching with TBAOH intercalation	4.35	23
V_2C–MXene	HF etching with TBAOH intercalation	384.6	24
Nb_2C–MXene	HF etching	0.00164	25
Mo_2N–MXene	Ammoniation of Mo_2C	2083	24
V_2N–MXene	Ammoniation of V_2C	4166	24
Mo_2TiC_2–MXene	HF etching with TBAOH intercalation	50	26
$Mo_2Ti_2C_3$–MXene	HF etching with TBAOH intercalation	100	26
Ti_2C–MXene	HF etching, free-standing disc	~2	27
	HF etching with hydrazine monohydrate intercalation (disc)	~0.178	28
	HF etching with TMAOH intercalation (free-standing film)	~200	29 and 30
	Fluoride based salt etching (LiF + HCl, free standing film)	6000–8000	30 and 31
	MILD method (free-standing film)	~8000	30
1T-MoS_2	Chemical exfoliation and intercalation	10–100	32
Graphene	Mechanical exfoliation	~2000	33
rGO	Hummers' method and thermal reduction	550	34

2.2 Hydrophilicity

The hydrophilicity of MXenes can be ascribed to their surface terminations such as hydroxyl, chlorine, or fluorine groups. Synthesis of MXenes using acidic-fluoride-containing solutions results in –O, –OH, or –F terminations, represented by the chemical formula $M_{n+1}X_n(OH)_xO_yF_z$.[35–37] The surface terminations on MXene are randomly distributed and the presence of the –OH group facilitates hydrogen bonding with water.[13] Being a hydrophilic material, $Ti_3C_2T_x$ MXene exhibits higher electrical conductivity when compared to solution-processed graphene.[38] Furthermore, the intercalation of cations during the synthesis process assists $Ti_3C_2T_x$ sheets to slide over each other by influencing their rheological properties and exhibiting a clay-like behavior.[38,39] The hydrophilicity and metallic conductivity of $Ti_3C_2T_x$ MXene allow them to form stable water-based conductive inks having a uniform dispersion without the need for any surfactants or additives.[40] Hence, MXenes enable easy processing of functional inks for different thin film fabrication methods such as printing, coating, and casting techniques to develop wearable sensors.

2.3 Ability to form free-standing films

Delamination of layered materials into individual layers is necessary to probe their characteristics in the 2D state. In its multilayer form, MXene exhibits two- to four-fold stronger interlayer interactions when compared to layered materials such as graphite or bulk MoS_2.[41] $Ti_3C_2T_x$ flakes with strong interlayer interactions assist easy formation of flexible films that demonstrate excellent electrochemical and piezoresistive properties. Different polar organic molecules such as hydrazine, urea, dimethyl sulfoxide (DMSO), or iso-propylamine, or large organic base molecules such as tetrabutylammonium hydroxide (TBAOH), choline hydroxide, or n-butylamine can be used as an intercalating agent during the MXene synthesis process. The intercalated MXene layers when subjected to mechanical vibration result in a colloidal solution of single to few-layer MXenes. Filtering of this solution forms a uniform film on the filter paper that can be easily peeled off after drying. The resulting free-standing film in the form of MXene 'paper' manifests superior flexibility and electrical conductivity and constitutes a potential candidate for wearable sensors. These free-standing films can be easily patterned into user-defined shapes and size, and their thickness and conductivity can be tuned by controlling the concentration of MXene in the solution. The unique 2D morphology of MXenes endorses them as the 'building block material' for various sensing applications.

2.4 Mechanical properties

The distinct compositions and versatile chemistry of MXenes bestow them with a variety of compelling mechanical properties which greatly complement other electrochemical characteristics. The mechanical properties are also influenced by the number of atomic layers in the MXene structure, determined by 'n' in its chemical formula $M_{n+1}X_n$. The flexibility, bendability, Young's modulus, stress–strain relationships, and fracture strength are the key mechanical parameters that need to be investigated since they play a vital role in the fabrication of wearable sensors. Borysiuk *et al.* have computationally studied the bending ability of MXene nanoribbons.[42] This is vital for body mountable flexible sensors as many wearable strain and pressure sensors work on the principle of bending of the sensing layer with respect to applied pressure. The bending rigidity (D) of the MXene layer increases with its thickness (h) which can be governed by the equation

$$D = \frac{Eh^3}{12(1-\gamma^2)}$$

where E is Young's modulus and γ is the Poisson ratio. MXene is one of the very few 2D materials that can produce flexible free-standing films, as detailed in the previous section. The elastic modulus of MXene along its basal plane is predicted to be over 500 GPa by first-principle studies.[43] Lipatov *et al.* have studied the mechanical properties of Ti_3C_2–MXene monolayer using the atomic force microscopy (AFM) indentation method as represented in Fig. 1A.[44] Further, Young's modulus of the Ti_3C_2 monolayer was calculated to be 330 ± 30 GPa and the breaking strength was 17.3 ± 1.6 GPa. The smaller value of Young's modulus obtained experimentally against the computational

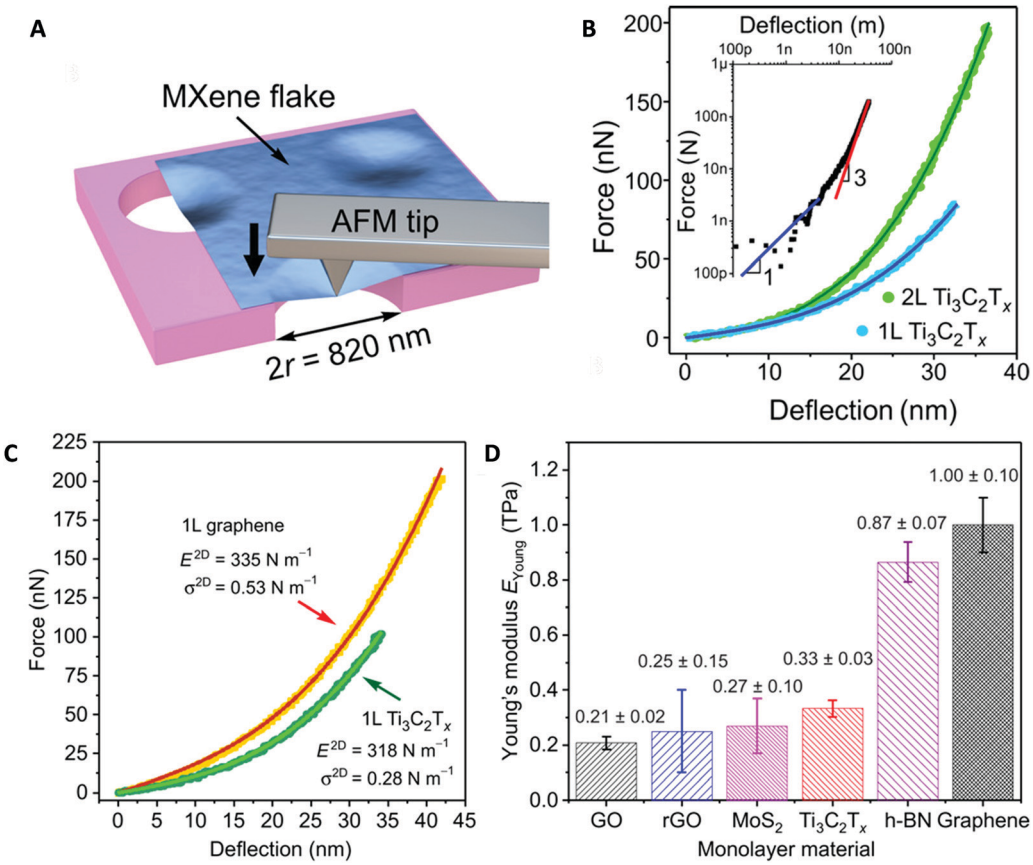

Fig. 1 Mechanical properties of Ti_3C_2–MXene: (A) the nanoindentation test was performed on suspended Ti_3C_2–MXene to measure the mechanical properties. A Si/SiO_2 substrate with prefabricated microwells was used to suspend Ti_3C_2–MXene and subjected to microforces using an AFM tip. (B) Force *vs.* deflection curves of monolayer and bilayer Ti_3C_2–MXene observed under AFM indentation. (C) Force *vs.* deflection curves of graphene and Ti_3C_2–MXene. The elastic modulus (E^{2D}) and stress in the sheets (σ^{2D}) of Ti_3C_2–MXene were less compared to those of graphene. (D) Young's modulus of various monolayer 2D nanomaterials: GO, rGO, MoS_2, h-BN, and graphene. Adapted under the terms of the CC-BY Creative Commons Attribution 4.0 license.[44] Copyright American Association for the Advancement of Science 2018.

method (~500 GPa) can be attributed to the presence of surface functional groups and mechanical defects.[44] A comparison of force *vs.* deflection curves for monolayer and bilayer Ti_3C_2–MXene is shown in Fig. 1B. Young's modulus of bilayer Ti_3C_2–MXene was found to be twice that of monolayer Ti_3C_2–MXene, suggesting strong interaction between layers possibly arising from the hydrogen bonding between the functional groups of Ti_3C_2.

In general, monolayer graphene is the strongest material known with a Young's modulus value of around 1 TPa. Force *vs.* deflection curves of pristine graphene and Ti_3C_2–MXene are compared in Fig. 1C. The elastic modulus (E^{2D}) and stress in the sheets (σ^{2D}) in monolayer Ti_3C_2–MXene are comparatively less than their graphene counterparts. These extreme properties of graphene are limited to mechanically exfoliated layers, and they have the disadvantage of poor solubility in many solvents and the small lateral size of individual layers. Interestingly, graphene oxide (GO) is a low-cost and scalable alternative to graphene. The presence of functional groups in GO makes it easily solvable in water and other solvents, and its ability to form monolayers of large lateral size provides added advantage in sensor fabrication. The monolayer of GO exhibits a young's modulus value of 200 GPa, 5 times less compared to that of pristine graphene due to its crumpled structure. A comparison of Young's modulus of MXene with that of pristine graphene, GO, rGO and MoS_2 is shown in Fig. 1D. MXene displays superior properties compared to solution-processed graphene (GO and rGO) and MoS_2. Albeit there are approximately 20 MXenes that can be synthesized, the mechanical properties of most MXenes are yet to be verified experimentally.

Flexible and stretchable strain sensors gained popularity in wearable platforms with diverse applications involving physiological health monitoring. However, the metal- and semiconductor-based conventional strain sensors exhibited a narrow sensing range ($\varepsilon < 5\%$) and low gauge factors (GF ≈ 2). The epidermal sensors are recommended to be of very low thickness such that they can be perfectly mounted on human skin for maximum strain sensitivity and accurate measurements. Interestingly, the stiffness of MXene films varies by changing the surface terminating groups. It is proven that –F and –OH terminations on MXene yield low elastic stiffness while –O termination results in MXenes of very high elastic stiffness.[45] Wearable sensors for monitoring physiological signals demand curvilinear shapes and adaptable elastomeric

substrates. Flexibility of MXenes with other tunable properties offer scope for building a stretchable device in accordance with the body architecture considering all the tensions at the surface level.

2.5 Electrochemical properties

The literature demonstrates the potential use of Ti_3C_2–MXene as an efficient electrode material for electrochemical energy storage and battery applications.[46,47] The presence of polar groups along with the large surface area of MXene offers prospects for further functionalization and anchoring of biomolecules (DNA, enzyme, protein, *etc.*) and plays a catalytic role in the fabrication of highly efficient biosensors.[48–50] Besides this, the large surface area and anti-bacterial properties[51] of MXene are predicted to be a better platform for immobilization of biomolecules. They increase the loading of biomolecules with the desired orientation and enhance the performance of biosensors in terms of sensitivity, detection limit, and stability. Similar to other 2D materials, Ti_3C_2–MXene also suffers from the restacking problem, limiting its electrochemical performance. The restacking of MXene layers eventually prevents ionic transport and minimizes the access of electrolytes to the active redox sites. This problem can be overcome by spontaneous intercalation of MXene layers using polar organic molecules, metal ions, and electrochemically active materials. For example, a range of mono- and multivalent cations such as Li^+, Na^+, K^+, NH^{4+}, Mg^{2+}, and Prussian blue can intercalate (chemically or electrochemically) and occupy electrochemical active sites on the MXene surfaces. The diverse chemistry and promising characteristics of MXenes serve as a sensitive interface and allow the detection of the analytes present in biofluids such as saliva, sweat, tears, and urine. Therefore, MXenes portray as a promising sensing material for the development of wearable electrochemical sensors.

2.6 Biocompatibility

Integration of MXene based wearable devices on the human body requires careful consideration of allergic reaction, toxic behavior, and biocompatibility studies.[52] These parameters need to be addressed during the experimental design for human trials. For long-term integration of MXene based wearable devices, the interface must be biocompatible for continuous monitoring of bio-signals (ECG, EMG, EEG, *etc.*) with a high signal-to-noise ratio. Otherwise, it may progressively increase the body impedance triggered by the immune response.[53] Recent studies have opened up the possibilities of use of MXene for theragnostic nanomedicine, biosensing, imaging, as an antimicrobial agent, and for cancer treatments.[52] MXenes have been reported as multifunctional theragnostic agents for efficient magnetic resonance (MR) and photoacoustic (PA) dual-modality imaging-guided photothermal therapy (PTT) against cancer due to their excellent biocompatibility which is a significant pathway.[54] MXenes facilitate the fabrication of mediator-free biosensors by enabling direct electron transfer between the electrode and bioreceptors and acting as biomolecule immobilization matrices to protect active proteins. The TiO_2–Ti_3C_2 nanocomposite was revealed to be an excellent immobilization matrix from spectroscopic and electrochemical studies, displaying compatibility towards redox protein and affording good stability and protein bioactivity.[55] These multifunctionalities of 2D MXenes with intriguing biochemical properties pave a new avenue for versatile sensing modalities in wearable biosensing applications.

3. Fabrication of the MXene sensing layer

Hydrophilicity and metallic conductivity project MXene as a well-desired candidate for fabrication of versatile wearable sensors towards biomedical applications. The presence of surface functional groups such as hydroxyl (–OH) and oxygen terminations (–O) provides a hydrophilic nature which enables MXenes to be dispersed into aqueous solutions and inks. These inks can be effectively utilized in realizing sensors using various approaches like drop-casting, screen printing, spin coating, extrusion printing, *etc.*, which are explained below in detail. The rheological properties of MXene dispersion at various concentrations were studied to set guidelines for these fabrication methodologies.[56] The substantial surface charges along with hydrophilicity allow MXenes to form dilute dispersions at low concentrations (<0.20 mg mL^{-1})[56] suitable for spray, dip or spin coating applications. Higher concentration slurries have also been reported to exhibit flowability at MXene dispersion up to 70 wt%. These high loading slurries obtained *via* swelling of multilayer MXene could be utilized for applications that demand high packing density and form 3D printable inks without any sacrificial additives that can be used for extrusion or inkjet printing.

3.1 Dip coating

In this method, a substrate is immersed in solution containing the coating material, soaked for a while, and pulled out, wherein the pulling speed dictates the thickness of the desired coating layer. To ensure that the substrate is uniformly covered with the coating material, it is completely immersed in the coating solution and then dried *via* heating or at room temperature. The amount of functional material deposited on the substrate depends on the absorption ability, surface properties of the substrate, and the concentration of the solution.

Yue *et al.* reported a porous MXene sponge network as a piezoresistive sensor.[57] Sponge being a widely available material is cost-effective and a good absorber of solvents. Its porosity coupled with high surface area and flexibility makes it an ideal candidate for fabricating body-mountable sensors. In the reported work, the dipping–drying method was adopted for sensor fabrication, wherein the sponge was dipped in MXene solutions of different concentrations and combined with polyvinyl alcohol (PVA) nanowires as a spacer. The fabrication process flow is demonstrated in Fig. 2A.

In another work, Guo *et al.* reported the fabrication of MXene based wearable pressure sensors using the dip coating method for human-machine interfacing.[58] The fabrication of

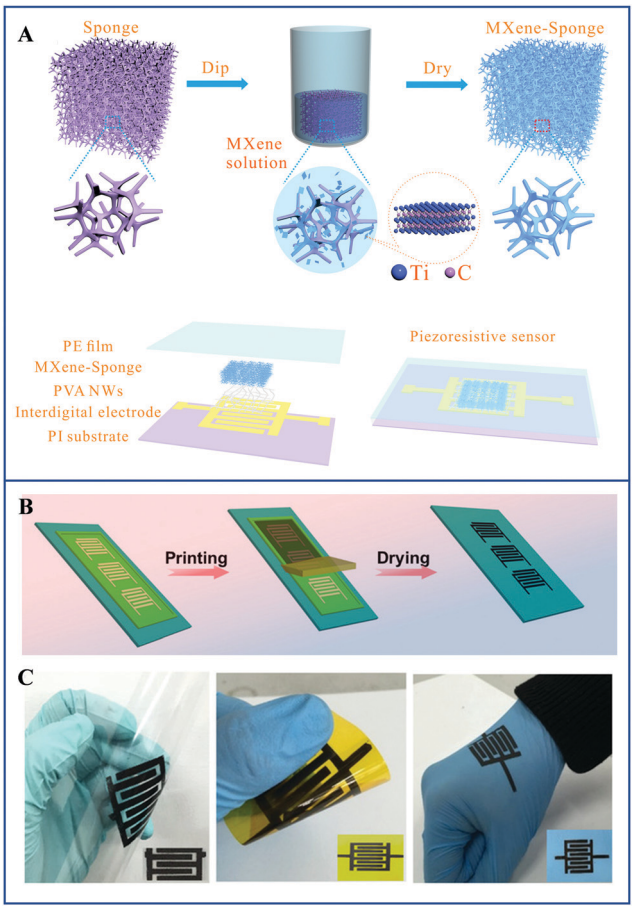

Fig. 2 MXene sensor fabrication *via* dip coating: (A) the dipping–drying method was adopted to fabricate a 3D hybrid porous piezoresistive sensor by dipping sponge in MXene solutions of different concentrations and combining with polyvinyl alcohol (PVA) nanowires as a spacer. The fabrication process flow is illustrated in the figure. Reprinted with permission from ref. 57. Copyright Elsevier 2018. (B) The screen-printing process is explained in detail. A mask of the desired shape was placed on the substrate and the MXene slurry was dropped on top. Printing was carried out by applying a squeegee at a specific velocity. The mask was later removed, and the pattern was dried to obtain the MXene film of the desired shape. (C) MXene films are printed on various substrates. Photograph displaying the excellent flexibility of screen-printed films. Reprinted with permission from ref. 60. Copyright John Wiley and Sons 2019.

the pressure sensor comprised of tissue paper as the base which was dip-coated in MXene solution and sandwiched between PLA films. Tissue paper was cut into the desired shape (a rectangular piece of size 0.6 mm × 0.8 mm) and immersed in MXene solutions of different concentrations. Sheet resistance decreased from 56.5 MΩ to 6.7 kΩ with the increase in concentration due to better connectivity between sheets. Solution concentration was optimized at 2.5 mg mL^{-1} for low sheet resistance, high-pressure sensitivity, and good repeatability. Porous tissue paper ensured uniform coating all over the substrate, owing to the strong adsorption and interconnected porous nature of paper. Similarly, Ma *et al.* fabricated piezoresistive strain sensors by dip-coating a flexible polyimide (PI) substrate in MXene solution.[59] MXene ink was optimized by dispersing MXene sheets in ethyl alcohol at a concentration of 250 mg mL^{-1}. The dip-coated sensor displayed a gauge factor of ~180 with a fast response time of ~30 ms. It is important to note that the number of coating layers is inversely proportional to the flexibility of the thin film. The increase in deposited 2D layers on the substrate reduced the flexibility of the sensor with the possibility of inducing cracks in the sensing film at high bending conditions. Therefore, a balanced approach is required to maintain the high sensitivity and flexibility of the device.

Dip coating ensured high electrical conductivity of films over a large specific area, large scale production and a low-cost fabrication process. However, this method has possible drawbacks such as requirement of a large volume of coating solution and high dependence on substrate adsorption and surface properties, and offers no flexibility in patterning.

3.2 Screen printing

Screen printing is a highly popular and versatile printing technique adopted by various industries like clothing, polymer, graphics, printed electronics, *etc.* Here, a permeable membrane is used to transfer the coating material (ink) onto the substrate with the help of a blade or a squeegee. Specific patterns are produced on the permeable membrane using a stencil that blocks inks from seeping through.

Yu *et al.* reported screen printing of nitrogen-doped MXene inks for energy storage applications.[60] The ink consisted of crumpled MXene-N nanosheets synthesized *via* the MF templating method. In the reported work, melamine-formaldehyde (MF) was added to the aqueous dispersion of MXene, which spontaneously wrapped MXene around the template to produce a crumpled structure. This procedure also doped MXene with nitrogen, thereby increasing the electrochemical activity of the resulting material through surface modification. The ink was stabilized by mixing super P, LA123 binder and DI water. The MXene slurry displayed shear thinning behavior where the viscosity of the fluid decreased with increasing shear rates. This property is essential to maintain a continuous flow of ink for the screening printing process. In a typical procedure, the screen printing mesh with the interdigitated pattern was obtained by the photochemigraphy method. The MXene-N slurry was dropped on top of the mesh and spread across using a squeegee that moved at a velocity of 2 m s^{-1}. The ink was transferred from the mask to the substrate forming an interdigital pattern, and then it was air-dried to get the final conducting structure (Fig. 2B). The films printed *via* this technique displayed superior flexibility as shown in Fig. 2C.

The screen-printing method can be successfully adopted to print MXene on various substrates such as PET, PI, paper, rubber, Al foil, copper foil, glass, and stainless-steel. This is a widely popular and cost-effective procedure that can be easily adapted to fabricate wearable devices for sensing applications.

3.3 Blade coating

Blade coating is an industrially adopted coating and printing process where the desired coating material is poured on the substrate. The excess material is removed using a blade to produce a uniform layer of coating on the substrate. The blade

moves along the length of the substrate at a specific height which determines the thickness of the coating layer. The ink is then annealed at a particular temperature. A similar strategy was employed by Zhang *et al.* to obtain free-standing films of Ti_3C_2–MXene.[61] The blade coating method was used to print additive-free MXene inks on a Celgard membrane (Fig. 3A), dried at 200 °C, and peeled off to produce free-standing films with highly stacked layers of MXene. However, the superior mechanical properties of single-layer MXene are usually not transferred to the macroscale due to the limitations in solution processing that result in smaller flake size and poor flake alignment. The group has discovered that increased lateral size of individual MXene flakes can produce highly aligned films when printed at the macroscale, thereby boosting their mechanical and electrical properties (Fig. 3C and D). Flakes of high lateral size can be achieved through certain modifications in the MXene synthesis process. Following the MILD technique, an average flake size of 10 ± 2 μm was reported by Zhang *et al.*[61] These flakes with large lateral size were carefully aligned into thin films of desired thickness *via* blade coating. The precise control over flake alignment played a vital role in determining the conductivity and strength of MXene films. Blade coating produced uniform films of 924 nm thick MXene, several meters in length with the highest tensile strength (568 ± 24 MPa) and Young's modulus (20.6 ± 3.1 GPa) reported for pristine MXene. The 214 nm film obtained *via* blade coating exhibited the highest electrical conductivity of 15 100 S cm^{-1}.

Another common technique to obtain free-standing films of MXene is *via* vacuum filtration.[62] However, the simplicity of the vacuum filtration method is overshadowed by the limitations to produce films of large lateral size, which mainly depends on the size of the filtration setup. Also, the alignment of MXene flakes in the vacuum filtration method is poor when compared to the blade coating method, as shown in Fig. 3B. Thus, the blade coating method produced dense packing of MXene flakes whose tensile strength was reportedly 30 times higher than that of vacuum filtered films. In addition to high tensile strength and conductivity, blade coated MXene films also displayed excellent flexibility. Fig. 3E shows the free-standing MXene film bent at different angles. The films were tested for stability under repeated bending conditions of 180° angle for 5000 cycles. The electrical resistance of blade coated films increased to a minimal value of ~0.4% after the cycling test indicating superior mechanical stability for bending (Fig. 3F). Therefore, it is anticipated that the large area free-standing films produced by the blade coating method have high strength and superior conductivity and can be used to fabricate flexible MXene sensors for wearable applications.

3.4 Stamping

Stamping is a process wherein a specific image or pattern is carved, engraved, or molded on a material, usually rubber. The mold is then coated with ink and pressed against a substrate or medium such that the desired pattern gets imprinted on the substrate. The stamping technique is widely used in the textile industry to imprint colored patterns on clothes. The method is effective in transferring ink patterns on a variety of substrates, including fabrics, paper, wood, plastic, and metals.[63] The stamping technique successfully

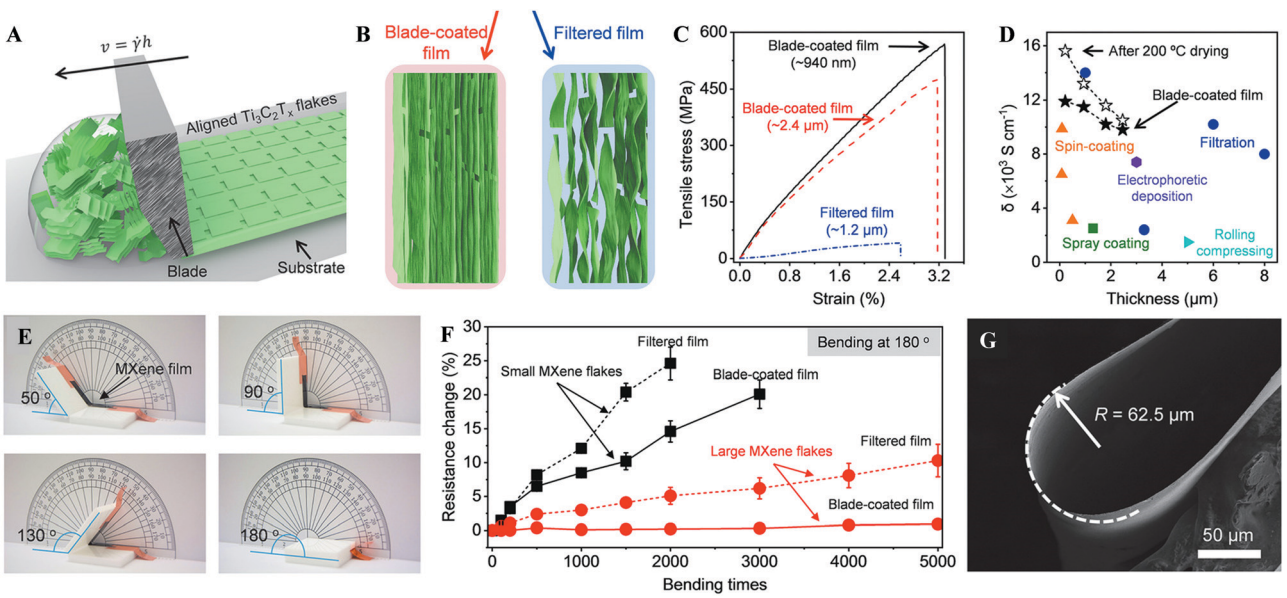

Fig. 3 Blade coating to produce free-standing MXene films: (A) illustration of the blade coating process where a blade moving on a substrate at a specific speed produced MXene film with highly aligned flakes. (B) Comparison of flake orientation in blade coated and vacuum filtered films. (C) The stress–strain graph indicates that blade coated films display much higher Young's modulus compared to vacuum filtered films. (D) The electrical conductivity of blade coated MXene films is compared with that of films obtained from other fabrication methods. The graph suggests that blade coated films exhibit superior conductivity, and it can be increased further by annealing at 200 °C for 6 hours. (E) A bending test of the free-standing MXene film done at specific angles confirms excellent flexibility. (F) Electrical stability of different MXene films bent at 180° for 5000 cycles. (G) 180° bending of the blade coated MXene film formed a radius of curvature of 62.5 μm as seen in the SEM image. Reprinted with permission from ref. 61. Copyright John Wiley and Sons 2020.

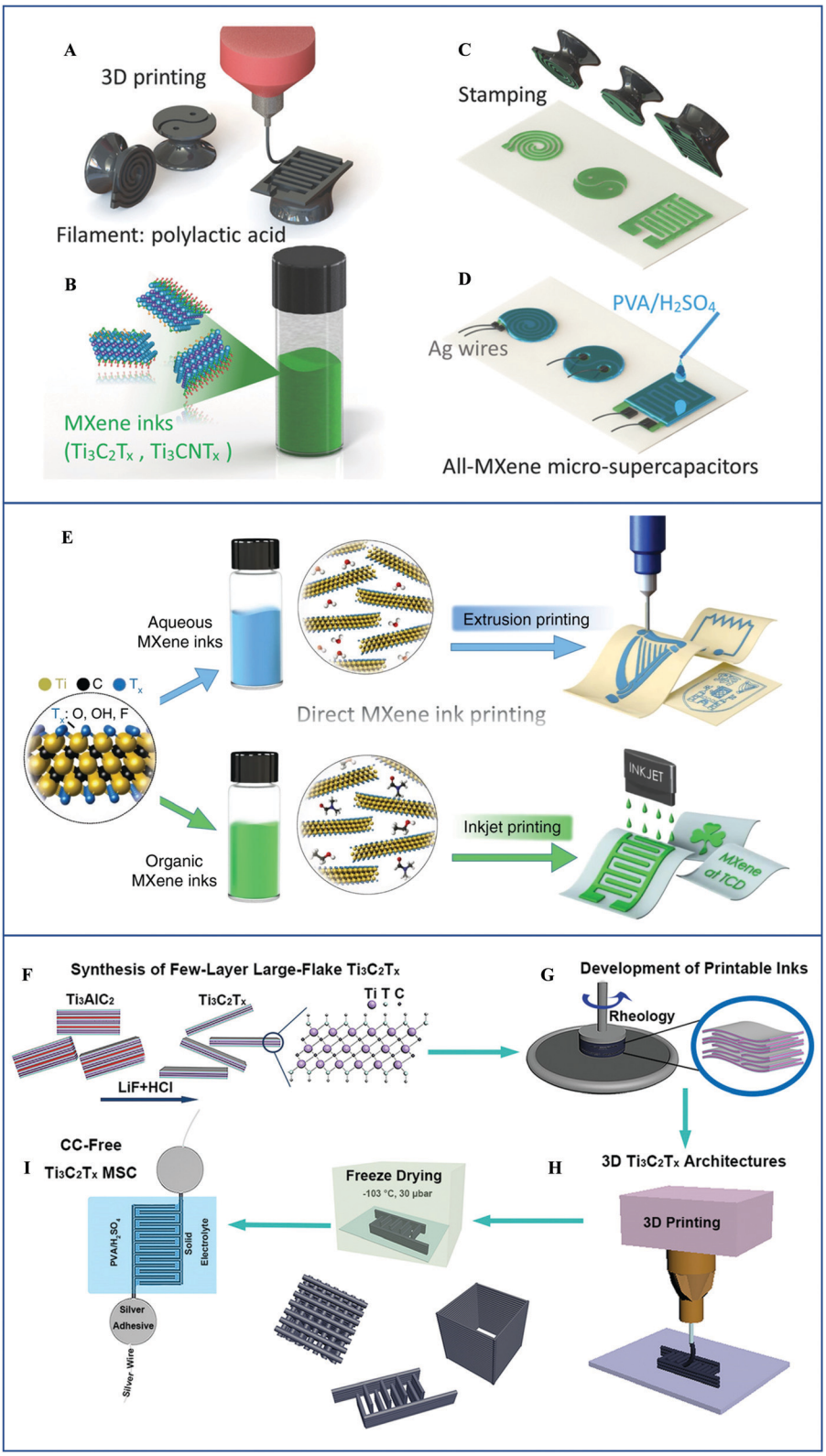

Fig. 4 Stamping, inkjet, and 3D printing of MXene: (A) stamping molds of different shapes were 3D printed specific to the given application. (B) $Ti_3C_2T_x$ and Ti_3CNT_x were synthesized and used as stamping inks. (C) MXene ink was brushed on the mold and pressed onto a flexible PET substrate. (D) The supercapacitors fabricated *via* stamping displayed superior performance. Reprinted with permission from ref. 38. Copyright John Wiley and Sons 2018. (E) Preparation of MXene inks in various solvents and demonstration of extrusion and inkjet printing. Adapted under the terms of the CC-BY Creative Commons Attribution 4.0 license.[70] Copyright Springer Nature 2019. (F) Schematic illustration of the process involved in the 3D printing of MXene devices. It starts with the synthesis of few-layer large flake $Ti_3C_2T_x$. (G) The rheological properties of MXene ink were tuned to make it suitable for extrusion printing. (H) 3D printing of MXene ink layer by layer in the required design. (I) Freeze drying at a specific temperature and pressure forms free-standing structures of MXene. 3D printed structures are used to construct energy storage devices. Reprinted with permission from ref. 71. Copyright John Wiley and Sons 2019.

yielded better results in fabricating various devices using graphene inks.[64] Unsurprisingly, rheological studies have shown that MXene inks can be tuned suitably for stamping. Zhang *et al.* have reported the fabrication of micro-supercapacitors by stamping MXene inks on a flexible substrate (Fig. 4A–D).[38] Different patterns were formed *via* 3D printing the desired stamp molds depending on the requirement. MXene ink was brushed on the mold and stamped on a flexible PET substrate. The stamped $Ti_3C_2T_x$ inks in the form of interdigitated micro-supercapacitors exhibited a high areal capacitance of 61 mF cm^{-2}. The 3D printed stamps with interdigitated electrodes achieved a spatial resolution of ~300 μm. For high concentration inks, the thickness of stamped MXene layers can be tuned by controlling the amount of ink brushed onto the 3D printed mold. The lowest thickness of ~100 nm was achieved by diluting the ink up to ten times and stamping it on an Al substrate. Stamping being a kind of transfer process, a certain value of film thickness is essential to form a uniform conducting layer depending on the substrate. Making ultrathin films is a limitation of this method. Additionally, the work also reported scaling up of the stamping process *via* fabrication of cylindrical stamps that can be cold rolled on a substrate to produce multiple patterns in minutes. Therefore, this process can be effectively used to fabricate wearable sensors on cloth or other flexible substrates suitable for body mountable sensing applications.

3.5 Spray coating

In this method, the coating solution is compressed and dispensed in the form of aerosols. When a pressurized liquid stored inside a container is released, it evaporates quickly outside the can, converting into mist by forming tiny droplets. The stream of dispersion is directional and can be controlled using a rotating nozzle. Uniformity of deposition can be achieved by changing the distance between the nozzle and the substrate and by tuning the spray pressure. Cai *et al.* demonstrated the fabrication of MXene/CNT nanostructures on an elastic (latex) substrate by the spray coating technique for strain sensor applications.[65] This layer-by-layer coating process involves spraying the MXene and CNT solutions on the latex substrate, followed by drying using a nitrogen gun. Individual layers of MXene and CNT were deposited one on top of the other alternatively multiple times until a continuous film of desired electrical conductivity and thickness is formed. Even though this method is cost-effective and scalable, the technique is not clean, and causes wastage of the coating material. Spray coating is also a time-consuming process, laborious and not suited for applications demanding very high patterning resolution.

3.6 Inkjet printing

With the advent of flexible electronics, inkjet printing evolved itself into a potential candidate for printing functionalized inks on a wide range of substrates such as plastic, cloth, paper, *etc.*[66] This low cost and scalable technique is suitable for fabricating strain gauges, transistors, LEDs, and photovoltaic devices.[67,68] Inkjet printing was widely used in graphene research to develop flexible electronics by dispersing graphene and its derivatives in adequate solvents.[69] In inkjet printing, the droplets of ink are propelled onto a substrate (provided with good surface adhesion) using a nozzle. The amount of ink dispersion and direction of flow can be controlled *via* a programmed mechanism. The functional inks must have key properties such as good dispersion in the solvent, low viscosity, ability to form droplets, good jetting capability without clogging the printer nozzle, and low surface tension for substrate wetting.

The inverse Ohnesorge number Z predicts the formation of stable ink droplets suitable for inkjet printing and is given by the expression

$$Z = \sqrt{\gamma \rho D}/\eta$$

where Z depends on surface tension (γ), density (ρ), viscosity (η), and nozzle diameter (D).[70] After ink propulsion, wetting of the substrate, uniform deposition, and drying of ink are crucialfor getting uniform films of desired conductivity. Zhang *et al.* introduced additive-free direct printing of MXene for energy storage applications.[70] The group demonstrated extrusion and inkjet printing of MXene inks prepared in both aqueous and organic solvents without any additives and surfactants (Fig. 4E). Furthermore, stable inks of MXene were formed using *N*-methyl-2-pyrrolidone (NMP) and ethanol as solvents for inkjet printing and an AlO_x coated polyethylene terephthalate (PET) substrate was used since the coating improved the wettability of the substrate for organic inks. Inkjet-printed MXene nanosheets were found to be well preserved even after 6 months. Resolution of printed patterns depends on the solvent and the type of substrate opted for fabrication. NMP ink on a PI substrate displayed better resolution for printing interdigitated electrodes (line width ~80 μm, gap ~50 μm, spacial uniformity ~3.3%) contrary to ethanol-based inks (line width ~580 μm, gap ~130 μm, spacial uniformity ~6.4%). On the other hand, substrates like glass and Kapton produced non-uniform films with NMP inks. Overall, the technique is highly flexible, fast, limits the wastage of materials, and provides good patterning resolution during printing.

3.7 3D printing

Additive manufacturing is a scalable alternative towards large-scale production of devices for industrial applications.[72] 3D printing is a process of rendering 3D structures of different shapes and sizes through sequential layer stacking of materials controlled *via* a computer. This method of fabrication is superior to previously discussed processes owing to its advantages that include greater design freedom, flexibility in design, design complexity, and optimized material usage. The versatility of 3D printing extends to the use of various materials such as polymers, ceramics, and metals.[73,74] Interestingly, studies have shown that 2D materials like graphene oxide and MXenes having a high aspect ratio and surface charges can be tuned with respect to their rheological properties and utilized as inks for extrusion printing.[56,75] Yang *et al.* have reported 3D printing of free-standing architectures of MXene for the first time towards energy storage applications (Fig. 4F–I). Initially, the as-prepared

MXene ink was analyzed for its rheological properties to understand its competence in 3D printing.[71] Optimizing the viscous and viscoelastic properties of ink is essential for it to flow easily through printer nozzles and retain the shape after extrusion. Earlier studies have observed a shear-thinning behavior in solutions of 2D materials[76,77] for which the viscosity recovery of shear-thinning MXene inks over time benefits the extrusion process. Viscoelastic fingerprints of MXene ink at 50 mg mL^{-1} exhibited an elastic modulus of 36 507 and a yield stress of 206 Pa, which are ideal for printing applications.[78,79] Once the ink was optimized, the group had successfully extruded various 3D structures using additive-free Ti_3C_2X, as shown in Fig. 4I. The extruded 3D structure was freeze-dried to protect the free-standing $Ti_3C_2T_x$ architecture. Ultimately, this method can be effectively utilized to fabricate wearable sensors of diverse sizes and shapes and can be employed for health monitoring applications.

4. Characteristics of MXene based wearable sensors

A wearable system in general consists of three components: (1) sensing electrodes, (2) data analysis unit, and (3) display unit. Limiting our discussion to the sensing and data collection units of soft bioelectronic wearable sensors, different possibilities are explored in detail. Although skin is termed as an information barrier for chemical changes happening inside, it is a gold mine of data to study muscle movements, sweat, and temperature combined with the functionalities of internal organs reflected onto the skin such as pulse, ECG, EMG, *etc.* It is essential for a wearable sensor to be flexible and robust, and have good adhesion to the human body. As we know, traditional sensors are bulky, heavy, and rigid, and hinder the movement of the test subject.[80] The advent of flexible electronics brought about sensors that are flexible, lightweight and skin conformal.[81] Moreover, wearable sensors are generally worn on the body for a prolonged period for continuous monitoring of vital parameters. These sensors are designed to provide a comfortable user experience while provoking no adverse effect on the body. Hence, wearable sensors must follow a few design criteria in order to display high sensitivity, durability, miniaturization, and robust build along with user comfort. The sensors fabricated using high-quality soft nanomaterials, particularly $Ti_3C_2T_x$-MXene, are known to improve their functionality and performance. Additionally, device packaging plays a crucial role in determining the flexibility, robustness, biocompatibility, and sensor adhesion to the human body. Electrical contacts are another parameter critical for wearable sensors to record accurate measurements of health signals. These criteria are elaborated in the following section.

4.1 Sensitivity

Selection of the MXene synthesis procedure, sensor architecture, and sensing mechanism plays a crucial role in achieving high sensitivity towards wearable measurements. MXene's flake size, electrical conductivity, and rheology influence sensitivity depending on the fabrication method adopted, as detailed in the previous section. The choice of a suitable substrate, the thickness of the sensing film, and the flexibility of the film determine the sensor response to external stimuli governed by the adopted sensing mechanism. Fabrication of the MXene sensing layer in the form of a free-standing structure, 2D coating, conductive polymer composite, or 3D assembly offers versatility in sensor design and high sensitivity specific to the given application.

Kedambaimoole *et al.* demonstrated the $Ti_3C_2T_x$–MXene resistor as a highly sensitive strain sensor in the form of an ultrathin skin mountable temporary tattoo ($\sim$20 μm thickness).[82] The free-standing film of $Ti_3C_2T_x$–MXene ($\sim$2 μm thickness) achieved *via* the vacuum filtration method facilitated ultrathin sensor fabrication. Its high strain sensitivity with a gauge factor of about $\sim$7400 has been attributed to the development of nanocracks and their propagation through the film due to applied strain. Gao *et al.* devised a piezoresistive sensor that measures the smallest changes in pressure by confining the MXene in microchannels.[83] The finger-like microstructure in the channel and the accordion-like architecture of MXene form a synergetic effect resulting in a highly sensitive sensor (99.5 kPa^{-1}) with a limit of detection of 9 Pa and a fast response of time of 4 ms. This body-mountable sensor demonstrated multi-functional characteristics, capable of sensing sound, micromotions, and acceleration in a single device.

4.2 Flexibility

Flexibility is an essential factor for wearable electronics since it is part of ergonomics. 2D materials in general possess inherent flexibility and hence are suitable for fabricating wearable sensors aimed at mounting on the curvilinear shape of the human body. Although MXene nanosheets are fragile when compared to other 2D materials like graphene,[84] with suitable packaging, they can be used as a flexible sensor for wearable applications.[85] The advantage of nano and 2D functional materials is that, though the lateral size of individual flakes is small, they can be uniformly coated on a flexible substrate and used as flexible sensors.[86] A similar strategy was adopted to fabricate different flexible devices using MXene.[65,87] These flakes, when deposited with sufficient thickness, form conducting films on flexible substrates. The act of bending or stretching induces strain in the MXene layers, forcing them to slide one on top of the other or develop cracks.[65] The change in the conductive pathways within the film due to bending can be measured as a function of induced strain, which is a prominent physiological signal to explore for health monitoring applications.

MXene's ability to form a free-standing film is explained in the earlier section (Section 2.3). The free-standing films fabricated using the blade coating method displayed high flexibility.[61] Metallic conductivity coupled with hydrophilicity enables MXenes to behave as filler materials for polymer composites. Ling *et al.* reported that MXene nanocomposites combined with polydiallyldimethylammonium chloride (PDDA) and polyvinyl alcohol (PVA) polymers offer commendable tensile strength for energy storage applications.[88] These free-standing polymer nanocomposites can be easily adopted in developing wearable biosensors. A recent

study has shown that $Ti_3C_2T_x$–MXene/CNT films obtained *via* LBL (layer by layer) assembly where the long hairy CNTs knitted the $Ti_3C_2T_x$ loose sheets into textile possess an enhanced and more ordered connection that improved the structure along with orderliness of layers and electronic pathways. As a result, this structure endowed MXene/CNT films with high polymeric elasticity favorable for stretchable sensing applications. The $Ti_3C_2T_x$–polyvinyl alcohol (PVA) composite on the other hand exhibited superior flexibility, large tensile strength and compressive strength when compared to isolated $Ti_3C_2T_x$ films.

4.3 Signal to noise ratio

Sensors in general are recommended to have a high signal-to-noise (SNR) ratio for accurate measurements. Wearable biomonitors continuously detect vital body parameters and they need to eliminate the influence of external noise generated from the body and surroundings for better health analysis. The human body is a complex and dynamic system under constant motion and is home to various mechanisms. Isolating a particular signal from the bunch of input stimuli is a requisite for any wearable sensing system. For example, sensors tracking artery pulse must suppress the response generated from muscle movements, sweat, and temperature fluctuations. Hence, a wearable sensing system must possess solid electrical contacts, a suitable skin mounting mechanism, and robust packaging to eliminate noise and improve SNR.

4.3.1 Electrical contacts. Electrical contact to a sensor enables the user to carry out various electrical measurements and record the device's response to a given stimulus. Wearable devices that are flexible and very thin demand flexible contacts to measure electrical response without causing any fluctuation in contact resistance. The metallic property of $Ti_3C_2T_x$–MXene aids the formation of ohmic contact with standard metal electrodes like gold, silver, and platinum which are predominantly used in the fabrication of piezoresistive strain sensors. Interdigital electrodes of gold sputtered on a substrate are commonly used for electrical measurements of MXene wearable devices.[57–59] To carry our accurate measurements, the contact resistance of the sensor also needs to be taken into account. In general, the electrical resistance of a thin-film sensor is given by

$$R_{\text{total}} = R_{\text{contacts}} + R_{\text{film}}$$

In piezoresistive strain sensors, the change in R_{contacts} adds up to the device sensitivity as explained by Li *et al.*[87] The work demonstrated pressure sensing using Ti_3C_2–MXene coated textile *via* the dip-coating method. Here, the MXene deposited textile was connected to the interdigitated electrode and pressure was applied. Under the influence of external pressure, the contact area between the sensing MXene film and the electrode varied. The change in the contact area altered the value of R_{contacts} thus changing the total device resistance which was proportional to applied pressure. Moreover, electrical contact for thicker MXene films can be drawn with metal wires attached using silver paste, conductive ink or slurry. Fabrication methods like 3D printing and stamping produce thick MXene films that require robust electrical attachments.[38,71] Silver paste may serve the purpose. Care must be taken while using silver contacts for flexible devices as dried silver paste solidifies and develops cracks that can hamper electrical measurements.

4.3.2 Sensor interface with the body. Wearable sensors are predominantly placed on the skin. It is known that the skin is the largest organ of the body which protects against pathogens, controls water loss, and regulates body temperature. The multifunctional epidermis consists of sweat pores and hair and is rough. The curvilinear shape of the skin along with its roughness dictates the need for soft, flexible, and conformal sensors. These sensors along with their packaging should be very thin to transfer maximum strain from the skin to attain high sensitivity. Epidermal electronics is a fully integrated system that is soft, flexible, and designed to match the physical properties of the human skin. When sensors are designed with skin-matching thickness, elastic moduli, and bending rigidity,[7,89] they seamlessly integrate onto the skin *via* the action of van der Waals forces alone, without the need of any adhesive layer.[90] Different polymers and hydrogels have been tried out as the packaging material to obtain better conformity and adhesion to skin.[91] Among these, soft materials such as the silicone elastomer Ecoflex have been popularly used as they display an Young's modulus (125 kPa) closely matching that of the human skin and allow a conformal skin interface.[80] It is recommended that the thickness of the sensor should be of the order of skin roughness to be skin conformal. The effect of device thickness is studied by changing the thickness of all layers proportionally.[92] Though many designs for wearable MXene sensors are reported, it is essential for them to be skin conformal to have better sensitivity, lightweight, and provide utmost user comfort. The surface morphology of skin is a crucial parameter to be studied for the design of skin conformal sensors. The skin surface can be represented by a sinusoidal waveform with skin roughness amplification h_{rough} and the wavelength λ_{rough} is given by the expression

$$y(x) = h_{\text{rough}}\left[1 + \cos\left(\frac{2\pi x}{\lambda_{\text{rough}}}\right)\right]\Big/2$$

These mechanical concepts are crucial for successfully building high-performance sensors that laminate skin. Various fabrication methodologies explained in earlier sections have demonstrated the ability to form ultra-thin MXene films with promising electrical and mechanical properties. Sensors designed using thin MXene sheets have a significant advantage in epidermal sensing applications.

4.4 Stability and durability

Ultrathin MXene films are fragile and are vulnerable to damage without mechanical support as wearable applications involve constant movement of body parts. Thus, proper packaging is mandatory for skin attachable devices. Additionally, MXene films are sensitive to humidity and temperature fluctuations.[93,94] To facilitate minimum possible oxidation, the standalone MXene films require robust packaging, containing barrier properties against oxygen, water vapor, dust, and other environmental fluctuations. In addition to the above-mentioned barrier properties, the packaging material should be soft and non-allergic to the skin. Wearable sensors demand ultra-thin packaging that is

ideally inexpensive, biocompatible, and biodegradable without hampering device sensitivity or flexibility. In recent work, a flexible PLA film was used to sandwich MXene coated tissue paper and was demonstrated as a wearable pressure sensor. The group reported that the sensor was environmentally friendly and biodegradable; when immersed in water, the sensor entirely degraded within two weeks.[58] Similarly, a thermoplastic polymer was used for packaging the MXene coated sponge deposited on a PI substrate. The packaging also ensured effective contact between the MXene sponge and the interdigitated electrodes deposited on the PI substrate.[57] However, further improvement in packaging structure and design is necessary to adapt transduction of new parameters such as respiration and biomarkers. One of the drawbacks of existing sensor packaging methodologies is the inability to integrate signal conditioning electronics with the sensing electrode as a complete system under a single package. Although significant improvements have been reported in the domain of sensor packaging over the recent years, further efforts are necessary to build wearable health monitoring systems with stable measurements and high SNR.

5. Sensing mechanism and applications of MXene wearables

The human body continuously undergoes several physical and chemical mechanisms to keep the body alive and functioning. These mechanisms involving the functioning of different organs generate various signals and actuations that can be sensed non-invasively to determine the person's health. Body-to-signal transduction in wearable sensors occurs *via* different mechanisms and it plays a significant role in fabricating highly sensitive health monitoring devices. The wearable sensing systems can be classified into physical and chemical sensors based on the body parameter under observation.

5.1 Physical sensors

Common physiological signals that are of interest include artery pulse pressure, body temperature, and strain induced from muscle movements. The bulk of MXene sensors reported to date are aimed at responding to the mechanical deformation caused by pressure and strain. Here are the major physical sensing mechanisms reported for MXene wearables.

5.1.1 Sensing mechanism

Piezoresistive based sensing. The majority of MXene strain/pressure sensors work on the principle of piezoresistivity. Any mechanical deformation of the conductive material induces a change in its electrical resistance known as a piezoresistive effect. When a conductive film is subjected to elongation or compression due to applied force, its resistance R changes according to the equation

$$R = \frac{\rho L}{A}$$

where ρ is the resistivity, L is the length, and A is the cross-sectional area of the conductor. Owing to the high sensitivity and simple design of piezoresistive sensors, the piezoresistive effect has been popularly adopted for wearable physiological sensing applications. High sensitivity is an important characteristic of wearable strain sensors which improves the signal-to-noise ratio during the detection of dynamic strain. Strain sensitivity is typically quantified with the gauge factor (GF) given by

$$\mathrm{GF} = \frac{\Delta R}{R_\mathrm{o} \times \varepsilon}$$

where ΔR is the change in resistance, R_o is the unstrained resistance, and ε is the strain. Along with high sensitivity, wearable resistive strain sensors must exhibit high flexibility to be mechanically reliable when mounted on the body, allowing for long-term use. Additionally, mechanical deformation under the application of strain can be of different types. The following are three main structural changes observed in MXene based strain sensors.

(i) Change in the interlayer distance. In general, allotropes of carbon, *i.e.*, carbon nanotubes (CNTs) and graphene, and their composites are widely used materials for wearable strain sensing applications since they exhibit no extensive plastic deformation when subjected to repeated strain. Since these materials possess high effective modulus ($\sim$1 TPa), the inner atomic structure hardly undergoes structural deformation to contribute to the sensitivity. These shortcomings have motivated the use of MXenes which have relatively large interlayer distances (3–12 nm) and hence permit easy interlayer atomic movement.[59] Fig. 5a shows the *in situ* TEM images demonstrating the reduction in the interlayer distance of MXene layers during compression. The change in the interlayer distance with respect to applied pressure leads to high sensitivity to subtle human physical activities. Further, Fig. 5a illustrates the interlayer movement mechanism of the MXene film under the influence of external pressure. The total resistance R_T of the sensor can be calculated from the equation

$$R_\mathrm{T} = R_1 + R_\mathrm{C}$$

where R_1 is MXene's part resistivity corresponding to the interlayers with an initial smaller distance, being a nearly unchanged resistivity under pressure, and R_C corresponds to interlayer resistance with varying layer distance as represented in Fig. 5a. The interlayer movement mechanism produced a high gauge factor (GF $\sim$ 180.1) and fast response ($<$30 ms) under various pressure conditions. The MXene-based process also exhibited good recovery performance with high repeatability (over 4000 cycles) without mechanical degradation.

(ii) Conductive network in the polymer matrix. MXene nanosheets dispersed in a polymer matrix such as PVA-based hydrogels exhibit a different kind of response to applied strain. Here, the strain sensitivity depends on the formation of new conductive pathways under the influence of external force.[38] Fig. 5b illustrates the network structure of the MXene nanosheets embedded within a polymer matrix. Upon application of force, as shown in Fig. 5b, the MXene composite material undergoes compressive deformation, reducing the gap between MXene sheets and creates new conductive pathways for the flow of electrons, and as a result, the resistance of the composite

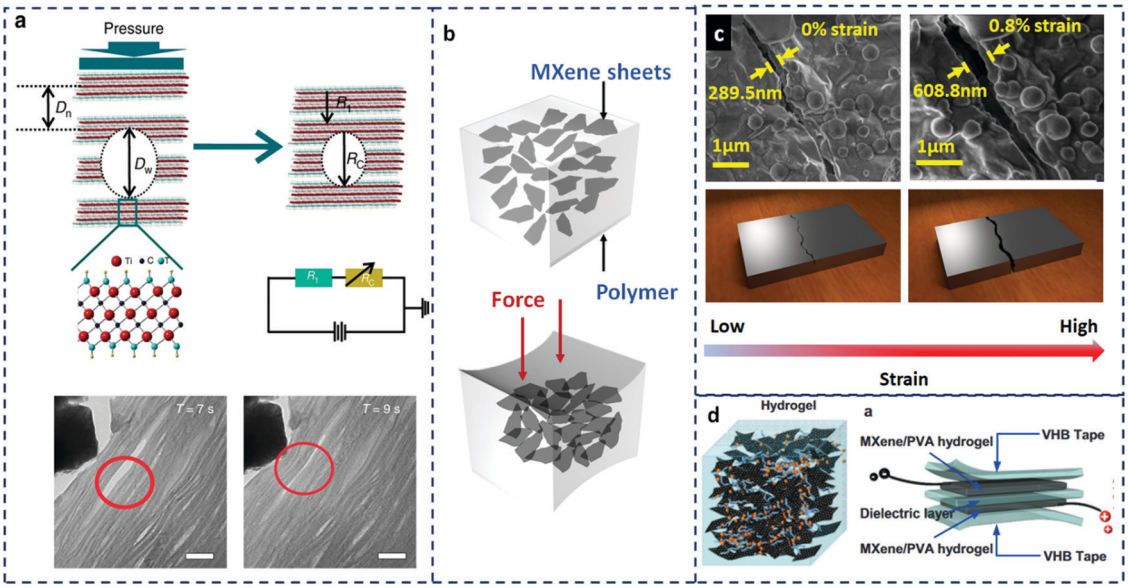

Fig. 5 Various sensing modalities for the MXene based wearable strain sensor. (a) The working mechanism of the MXene strain sensor with varying interlayer distance. External pressure decreases the wider gap between MXene layers (D_W) while the narrow interatomic distance D_n undergoes a smaller compression. This compression of MXene sheets results in a change in the resistance of the device as represented in the figure. Adapted under the terms of the CC-BY Creative Commons Attribution 4.0 license.[59] Copyright Springer Nature 2017. (b) Randomly oriented MXene nanosheets in a polymer matrix form new conductive pathways upon application of force. The sensor experiences a relative change in sensor resistance with respect to the magnitude of force applied. (c) SEM images of the freestanding MXene film illustrating the crack propagation mechanism under the influence of lateral strain. As the strain value increases, the gap between the crack edges widens, thereby increasing the sensor resistance significantly. Reprinted with permission from ref. 82. Copyright American Chemical Society 2020. (d) MXene-PVA hydrogel for the fabrication of stretchable capacitor electrodes. A dielectric layer sandwiched between MXene electrodes acts as a capacitor whose capacitance changes with the applied strain. Reprinted with permission from ref. 95. Copyright John Wiley and Sons 2019.

decreases. When the force is released, due to the elastic nature of the polymer in the composite, the spacing between MXene nanosheets expands and consequently increases the resistance. Similarly, the MXene layer deposited on porous substrates with high elasticity and internal surface area such as sponge, paper, *etc.*, also exhibits a similar strain sensing mechanism.[57,58] The 3D synergetic structure of the substrate material experiences structural deformation upon application of force. This changes the contact resistance between MXene conductive nanosheets resulting in a change in device resistance.

(iii) Generation and propagation of nanocracks. A new type of working mechanism was observed in MXene based wearable sensors where several nanocracks were developed on the surface of the sensing layer, and their width was varied to achieve a tunable resistance change upon application of tensile strain.[82] The stress developed at the MXene–polymer (PDMS) interface resulted in the generation of nanocracks and their density and spacing were controlled by stretching them in a particular direction. Fig. 5c shows the SEM images of freestanding MXene films where the nanocrack can be visualized under different strain conditions. Upon application of strain, the gap between the crack edges increases and causes a hike in device resistance. When the strain is released, the gap reduces, and the crack edges come in contact with each other to decrease the resistance. The difference in the elastic moduli of the MXene film and polymer substrate influenced this sensing mechanism to achieve very high strain sensitivity (GF $\sim$ 7400).

Capacitive based sensing. Apart from the piezoresistive effect, the capacitance-based approach was also demonstrated for wearable strain sensing applications.[95,96] Conductive MXene sheets were used to fabricate electrodes for capacitors whose capacitance was changed with the application of strain. As elasticity is an important form factor for the fabrication of wearable electronics, MXene–polymer composite (PVA hydrogel) electrodes were developed with high stretchability and self-healing abilities. The MXene–PVA hydrogel prepared to fabricate stretchable capacitor electrodes is shown in Fig. 5d. The MXene based electrodes with a dielectric layer sandwiched between them form a simple capacitor structure, as shown in Fig. 5d. Capacitance C of a standard capacitor is given by the equation

$$C = \frac{\varepsilon A}{d}$$

where ε is the dielectric constant of the material, A is the area of the electrodes and d is the distance between the electrodes. Under the influence of strain, the dimensions of stretchable MXene electrodes and the distance between them vary, leading to a change in the capacitance of the sensor. This mechanism while also being highly repeatable was used for E-skin applications for physiological monitoring.

5.1.2 Applications of physical sensors

Pulse monitoring. Arterial palpation due to opening and closing of the aortic valve is known as pulse and the arterial pulse is the most fundamental sign of clinical life. A trained fingertip can feel artery pulse on different locations of the

human body like wrist, neck, groin, knee, *etc.* The measure of artery pulse per minute determines the heart rate. A pulse wave consists of two major components: a forward-moving wave caused by the contraction of the heart, known as the systolic component, and a reflected wave originated by relaxation of the heart, also known as the diastolic component. A typical pulse waveform consists of percussion, tidal waves occurring during systole and the dicrotic peak arising during diastole, as shown in Fig. 6A. These waves provide valuable information regarding the heart and its functionalities. Analysis of different pulse components provides the details regarding a person's age, activity mode, and heart-related diseases.[97] Currently, several types of sensors are used to acquire the pulse signal that works on a different working mechanism such as piezoresistive sensors, piezoelectric sensors, capacitive sensors and infrared sensors.[8,98–101] MXene based strain sensors that work on the principle of piezoresistivity were employed to detect artery pulse with high sensitivity and precision. Various fabrication methods were adopted to make pulse detectors using MXene. Fig. 6B demonstrates the response of the MXene tattoo sensor to variation in strain caused due to artery pulse.[82] The ultrathin sensor fabricated *via* laser patterning of the free-standing MXene film was highly skin conformal, resulting in high sensitivity to artery pulse. Zhang *et al.* demonstrated pulse sensing using MXene and polymer composite-based strain sensors.[102] In this work, a composite hydrogel was prepared by mixing MXene with crystal clay which consists of PVA, water, and dehydrating additives. The M-Hydrogel, as they call it, exhibited excellent stretchability, self-healing ability, and good adhesion to human skin. The presence of abundant functional groups in conductive filler MXene formed a polymer-clay network structure with dense polymer chains which resulted in good elastic properties and stretchability. Besides, the large number of functional groups also increased hydrogen bonding in the composite structure thereby contributing to self-healing and adhesion properties. The M-hydrogel was mounted on the wrist to measure radial artery pulse. The pulse waves exerted strain onto the hydrogel which caused an increase/decrease in the contact area of MXene sheets, thereby changing their electrical resistance. Parallelly, an MXene/RGO aerogel was fabricated using a freeze-drying method as a piezoresistive strain sensor and its ability to sense artery pulse was studied.[103] This fast response and highly sensitive sensor was effective in recording human pulse and precisely distinguishing percussion wave and diastolic waves. The sensor was also successful in monitoring jugular venous pulse when it was placed on the neck. Another work related to a MXene based pulse sensor was reported by Shi *et al.* where a sensor fabricated

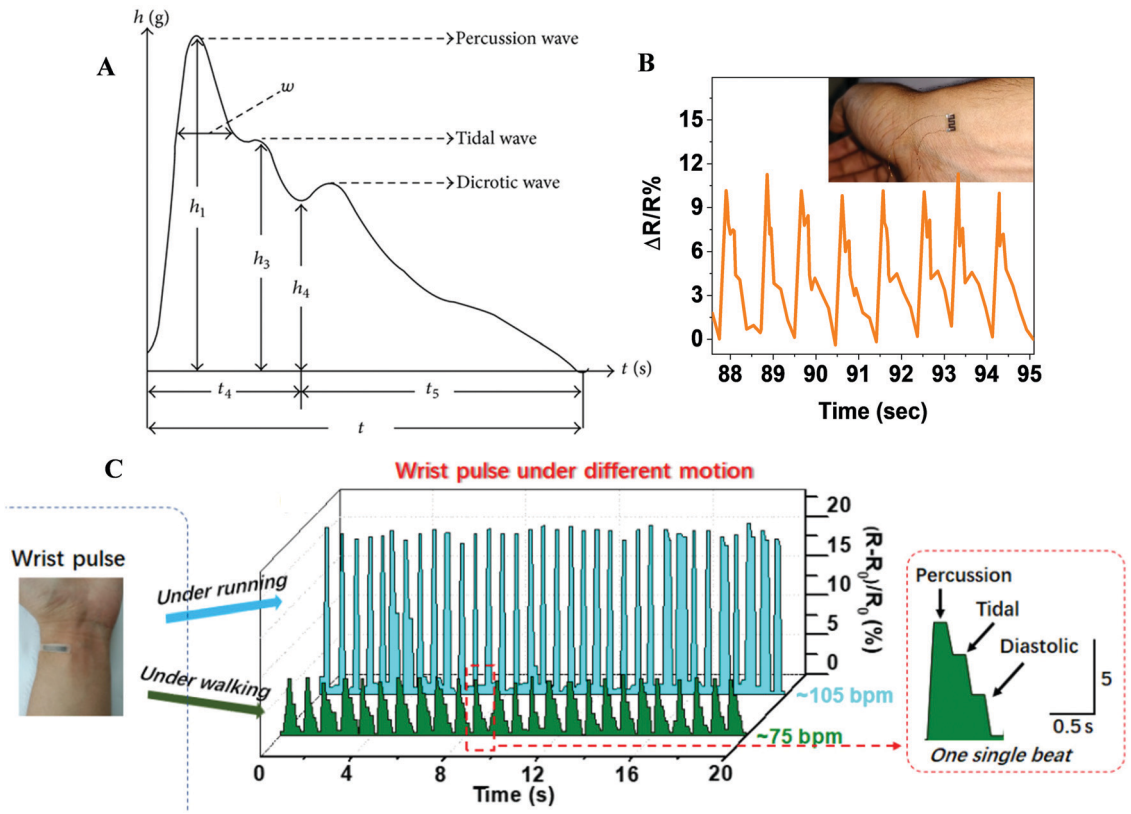

Fig. 6 Artery pulse sensing using MXene: (A) illustration of the typical artery pulse waveform consisting of percussion, tidal waves occurring during systole and the dicrotic peak arising during the diastole phase of the cardiac cycle. Reprinted with permission from ref. 97. Copyright American Chemical Society 2017. (B) The response of the MXene tattoo sensor for strain variations due to artery pulse. Reprinted with permission from ref. 82. Copyright American Chemical Society 2020. (C) $Ti_3C_2T_x$–Ag NW-PDA/Ni^{2+} strain sensor detecting the heart rate of a female subject walking at two different paces. Reprinted with permission from ref. 104. Copyright American Chemical Society 2018.

via the brick-and-mortar architecture was used for recording human artery pulse. The sensing element consisted of Ti_3C_2–Ag NW-PDA/Ni^+ gel-like inks screen printed on a polyurethane substrate and the sensor exhibited a high gauge factor for pressure measurements.[104] This ultra-thin and stretchable sensor was carefully mounted on the wrist and a single heartbeat was analyzed where the sensor recorded diastolic, tidal, and percussion components of pulse accurately (Fig. 6C). The wearable sensors fabricated using MXene were highly sensitive and repeatable. However, for continuous monitoring, incorporating one-time use sensors with environmentally friendly packaging material is extremely important. In this context, an MXene based biodegradable wearable sensor is reported to be stable for up to 2 weeks.[58] Robust substrates with firm packaging were used for the fabrication of sensors that are meant for long-term use.[38,57] Accordingly, high sensitivity and a wide range of strain sensing enable them to utilize a single sensor for multiple applications.[38,59]

Human activity monitoring. Electromyography (EMG) traces the electrical activities of muscles and records human muscle movements, which are essential for various biomedical applications. It also plays a vital role in athletic and prosthetic applications which could consequently pave the way for human-machine interfacing in the field of robotics. Moreover, accurate measurement of various muscle movements is possible using body mountable strain sensors. The discovery of CNT and graphene has revolutionized the flexible and wearable sensing domain as they display exceptional physical and electrical properties. The high electrical conductivity and flexibility of these materials aided the fabrication of complex structures on flexible substrates. The 1D CNTs form a highly interconnected network structure creating multiple conducting pathways for the flow of electrons. Upon application of strain, the network structure deforms, changing the resistance of the sensing layer proportional to induced strain.[105] This mechanism also provides high sensitivity compared to thin-film metal strain gauges. The orientation of CNT correspondingly plays a role in determining sensitivity and the operating range of the sensor.[106] A similar mechanism was introduced into making graphene-based flexible strain sensors. Conductive 2D layers of graphene slide over each other when subjected to strain. The change in the overlapping area modified the conducting pathways thereby varying the sensor resistance.[107] The flexible graphene monolayers provided better mechanical strength to the sensing layer thereby increasing the strain sensing capacity at higher strain values. The advantages of CNT and graphene were combined by fabricating graphene–CNT composite sensors to achieve higher sensitivity, a wide range, and robust design.[108,109] Likewise, high electrical conductivity is beneficial in utilizing the MXene as a filler material for polymer composites to fabricate sensors with superior flexibility. Piezoresistivity is the driving mechanism behind the MXene sensor's ability to respond to strain. The sensor attached to a specific part of the body when moved comes under the influence of strain. Such a strain mechanically deforms the flexible MXene layer thereby changing the electron conduction pathways. The change in the electrical resistance of the sensor is proportional to the applied strain. Human activity monitoring involves a wide range of measurements such as facial expression sensing, voice recognition, gesture sensing, movements of the arm and leg, and tracking feet movements. Facial expression and vocal cord movements fall under a lower strain regime, whereas muscle and joint movements of hand and legs involve recording of high strain values. Sensors need to exhibit a wide sensing range along with high sensitivity at low strain values for measurement of diverse body movements. A few such applications are discuss below:

(i) Facial expressions. Movements of muscles beneath facial skin mainly to convey emotions are known as facial expressions. Several facial muscles work together to constitute different facial expressions. Understanding and studying these expressions will benefit the emerging technologies in the field of machine learning, robotics, and human-machine interfacing. Moreover, tracking a person's expression also has biomedical applications such as monitoring the recovery from paralysis, brain injury, *etc.* In this context, the movement of the eyes is an important part of the display of emotions. Fig. 7A reports the use of MXene sensors for these applications. A MXene sensor was attached to the corner of the eye to track the opening and closing of eyelids such that the blinking rate could be analyzed to determine if a person was lying.[59] Furthermore, a MXene strain sensor was used to study the movements of cheeks which express happiness and sadness, basically being the key emotional states of humans (Fig. 7B).[59] A M-Hydrogel sensor attached on the eyebrows to record expressions is detailed in Fig. 7C.[102] A pressure sensor mounted on the cheek to monitor occlusion (Fig. 7D)[58] was also reported.

(ii) Voice recognition. Humans produce sound using their vocal cord to communicate and express emotions. The mechanism of voice production involves pumping of air from the lungs, vibration of vocal cords, and modulation and control of the voice depending on the scenario by articulators like tongue, cheek, and lips. The act of talking, singing, yelling, screaming, *etc.*, necessarily requires the production of sound. Generally, microphones are used to record, convert, and understand the different frequencies produced by humans to decode and comprehend the information they carry. Interestingly, strain sensors attached to the neck can be used to recognize the voice, following which MXene based sensors are mounted on the neck to study different sounds (Fig. 7F). The movement of Adam's apple and vocal cords induces strain in the wearable sensor causing a change in the resistance thereby producing unique patterns for different words (Fig. 7G–I).[102,103] The MXene sensor was used to record the act of swallowing and gulping for medical purposes.[58,59] The sensor attached to the neck also recorded breathing variations, as shown in Fig. 7E.[57]

(iii) Motion and gesture sensing. Gesture sensing is an important part of human-machine interfacing, and medical and athletic applications involving monitoring of muscle damage recovery, fractures, *etc.* Motion sensing involves a frequent and wide range of movements of muscles and joints. The sensor meant for such applications must be flexible and

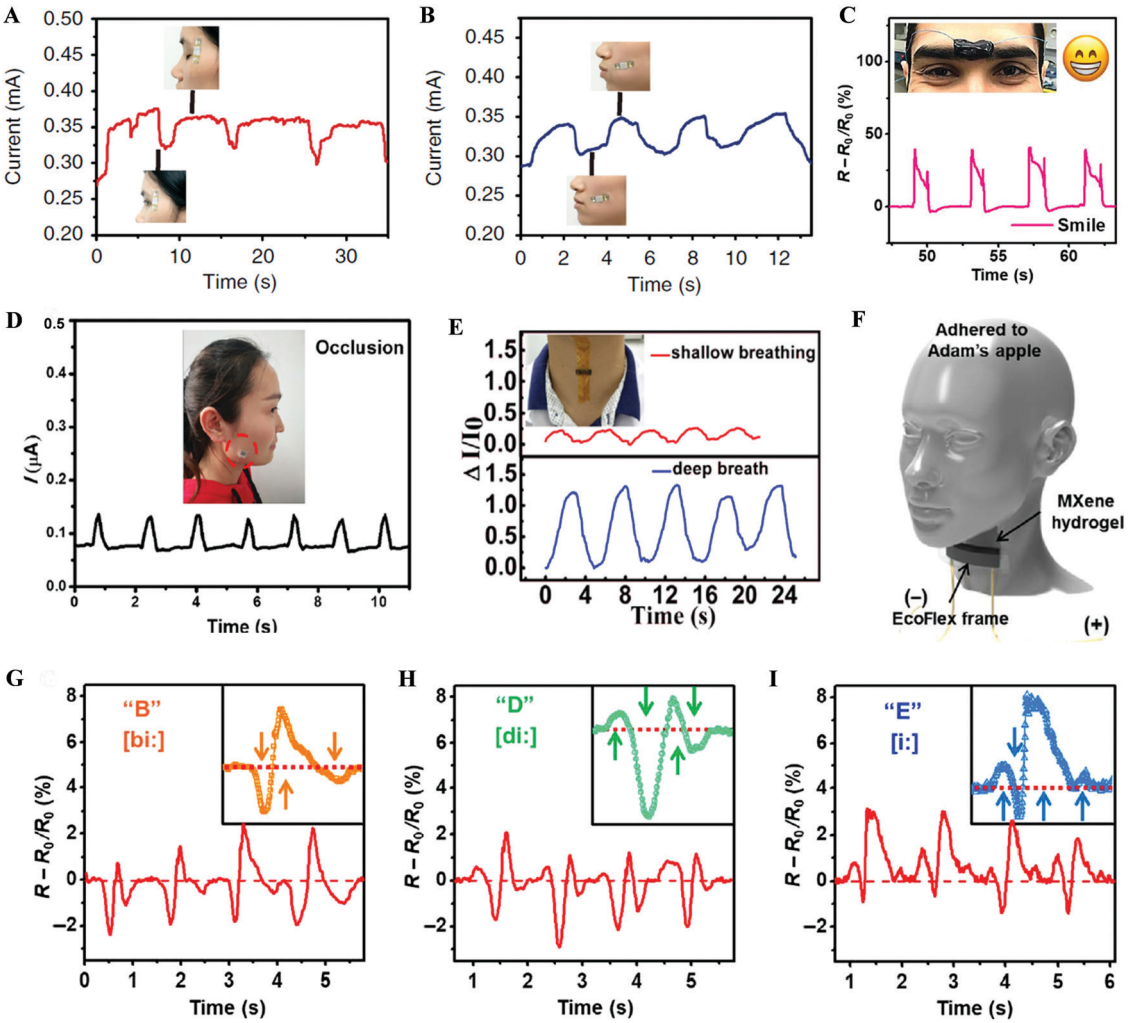

Fig. 7 Analysis of facial expressions and voice patterns: (A) MXene sensor attached to the corner of the eye to track opening and closing of eyelids to determine the blinking rate. (B) MXene strain sensor monitoring the movements of cheek muscles that express happiness and sadness, the key emotional states of humans. Adapted under the terms of the CC-BY Creative Commons Attribution 4.0 license.[59] Copyright Springer Nature 2017. (C) MXene–Hydrogel sensor attached on the eyebrow to determine different facial expressions. Adapted under the terms of the CC-BY Creative Commons Attribution 4.0 license.[102] Copyright American Association for the Advancement of Science 2018. (D) MXene coated tissue paper mounted on the cheek to determine occlusion. Reprinted with permission from ref. 58. Copyright American Chemical Society 2019. (E) MXene sponge 3D hybrid sensor attached on the neck to record the breathing patterns of the subject. Reprinted with permission from ref. 57. Copyright Elsevier 2018. (F) Schematic illustration of the sensor adhered to Adam's apple for voice sensing. (G–I) Different sounds produced by the vocal cord exerted specific strain on the MXene hydrogel sensor and created unique patterns in the *R vs. T* graph. Adapted under the terms of the CC-BY Creative Commons Attribution 4.0 license.[102] Copyright American Association for the Advancement of Science 2018.

highly durable. The sensor packaging should effectively suppress noise from various other parameters such as sweat and temperature. A wide variety of motion sensors were designed and fabricated utilizing the outstanding characteristics of nanomaterials like carbon nanotubes and graphene.[110–112] Flexible and wearable smart fabrics are becoming increasingly popular in healthcare and motion monitoring because of their potential applications in stretchable electronics. Recent work by Kedambaimoole *et al.* demonstrated the fabrication of flexible sensors using graphene for gesture sensing applications.[113] A highly stretchable sensor designed from dry spun CNT on an Ecoflex substrate was used to study human motion sensing.[105]

With the invention of MXene, researchers have found new ways to develop strain and pressure sensors. These sensors were utilized to study motion and gesture sensing. MXene coated 3D hybrid sponge was used as a strain sensor to determine finger movements as shown in Fig. 8A.[57] The sensor was attached to the finger joints and a change in current upon finger bending was monitored. A MXene-hydrogel composite sensor attached to the knuckles was capable of sensing gestures, as shown in Fig. 8B.[102] More complex gestures involving full hand motions like "zero," "one," "two," "three," "four," and "five" were sensed as they yielded a distinct resistance value, and the signals were fully recoverable. As MXene based sensors possessed high flexibility, sensitivity, and a wide range

of strain measurement capabilities, full-range monitoring of human activities could be widely explored. These sensors can be used to predict the potential health status of patients; Fig. 8C illustrates a MXene pressure sensor attached to an arm muscle to detect radial muscle contractions which occur through fist movements.[58] They are remarkably useful for physical training and also to cure muscle damage. Further, it is reported that flexible MXene sensors attached to muscles and elbow joints (orthopedic applications) and sealed with a transparent tape could record bending–straightening of joints easily, as shown in Fig. 8D. Furthermore, Fig. 8E illustrates the *I vs. T* response for ankle bending which yielded accurate measurements due to its credibility.[59] Monitoring of knee bending during walking to analyze body posture experiences large strain variations and such sensors demand high stretchability and working range. The $Ti_3C_2T_x$-Ag NW-PDA/N^{2+} composite sensor fabricated *via* the brick-and-mortar architecture could precisely measure motion signals under more vigorous movements like running.[104] Fig. 8F demonstrates a sensor attached to the knee for tracking the step counts of a woman moving at two different paces, first walking at 40 steps per minute and then running at 80 steps per minute. Utilizing the know-how approach of MXene based sensors and focusing on the specific application for in-depth studies may pave the way to address various unnoticed questions. Therefore, it is an attractive choice to incorporate sensors onto the body for motion sensing which can collect and process a variety of broad-range biomonitoring data.

5.2 Chemical sensors

5.2.1 Electrochemical sensor. There is a growing interest in the non-invasive measurement of metabolites and electrolytes through human body fluids (sweat, saliva, *etc.*).[114,115] Compared to physical sensors, wearable electrochemical sensors have the potential to continuously measure (bio)chemical markers such as glucose, pH, cortisol, electrolyte, *etc.*, of individuals that help in managing health and fitness. Electrochemical sensors are known to operate at low potential, and thus consume low power, and are safe for wearable applications. Further, ease of miniaturization, low cost, fast response time, and versatility of integrating with wearable electronics make them promising candidates for body mounting. In the fabrication of wearable electrochemical devices, transducer materials play a vital role in sensor performance such as sensitivity, selectivity, detection limit, *etc.* We have discussed the electrochemical properties of $Ti_3C_2T_x$–MXene in Section 2.5. These properties along with an understanding of the sensing mechanism are essential for the design and fabrication of wearable electrochemical sensors. Basically, electrochemical sensors use electrodes to translate a chemical reaction into an electrical signal. In addition, transducer materials are used to improve the performance of these electrodes, as well as to immobilize bioreceptors (enzyme, antibody, aptamer, *etc.*) efficiently without hindering their activity. Therefore, transducer materials are expected to have a high electrical conductivity that could measure small electrical changes at the electrode–electrolyte interface. To the best of our knowledge, there is one report to

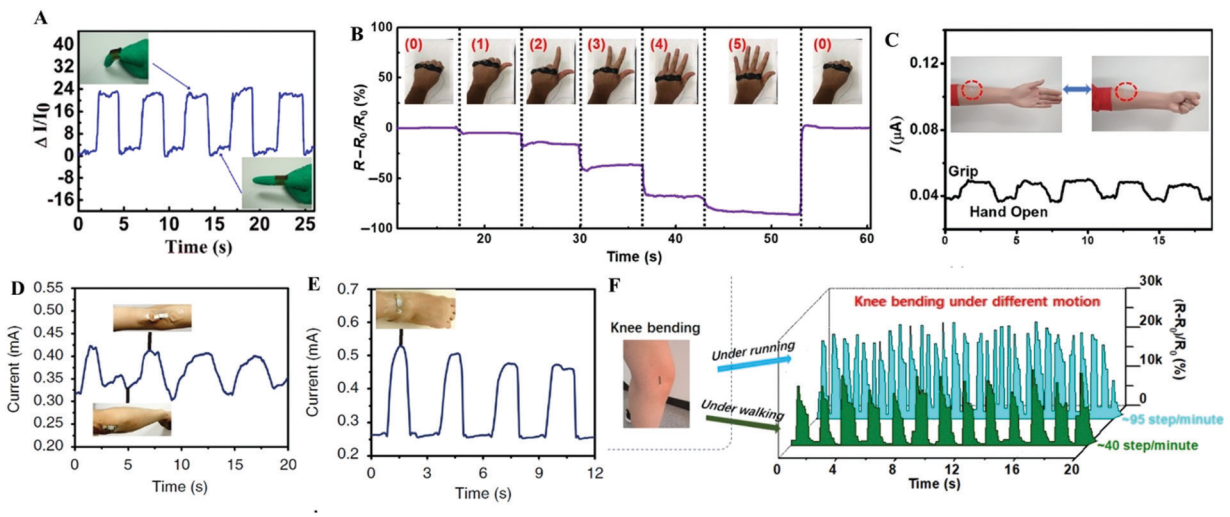

Fig. 8 Monitoring the movement of hands, legs, and feet. (A) MXene coated 3D hybrid sponge attached to the index finger and subjected to periodic bending and straightening movement. The real-time current response generated a stable waveform. Reprinted with permission from ref. 57. Copyright Elsevier 2018. (B) Attaching M-hydrogel onto the index finger reflected a 20% resistance change when the finger was bent. Under both fast and slow bending motions, the signal was stable and also, full hand motions could be readily detected by adhering M-hydrogel to the knuckle. Adapted under the terms of the CC-BY Creative Commons Attribution 4.0 license.[102] Copyright American Association for the Advancement of Science 2018. (C) MXene/tissue-paper-based pressure sensor was attached to an arm muscle with the help of medical tape and employed to detect radial muscle contraction. Reprinted with permission from ref. 58. Copyright American Chemical Society 2019. (D and E) The sensor is directly attached to the muscle joint and then is sealed with transparent tape thereby recording the bending release movement of the elbow and ankle. Adapted under the terms of the CC-BY Creative Commons Attribution 4.0 license.[59] Copyright Springer Nature 2017. (F) $Ti_3C_2T_x$–Ag NW-PDA/N^{2+} sensor can steadily detect the bending of the knee under vigorous movements like running and walking. Reprinted with permission from ref. 104. Copyright American Chemical Society 2018.

date that uses a $Ti_3C_2T_x$–MXene based electrochemical platform for wearable sensor applications.[49] In this work, $Ti_3C_2T_x$–MXene and Prussian blue composites were used as a highly efficient electrochemical indicator for the detection of glucose and lactate in sweat. One of the significant challenges in sweat-based enzyme sensors is poor sensitivity and limited detection range because of oxygen deficiency in sweat. To address these issues, a solid–liquid–air interface based biosensing patch (electrode) was designed using the CNTs/Ti_3C_2/PB electrode (CNTs are used to provide mechanical support). The patch was supported by super-hydrophobic carbon fibers (CFMs), which helped in preventing the electrode from wetting and facilitated oxygen diffusion from the bottom surface to the top of the biosensor patch where the enzymes were immobilized (Fig. 9B). The interaction with the analyte solution formed a solid–liquid–air interface and provided a constant oxygen-rich environment to the enzymes immobilized over the electrode (CNTs/$Ti_3C_2T_x$/PB/CFMs). This resulted in superior sensitivity (35.3 μA mm^{-1} cm^{-2} for glucose and 11.4 μA mm^{-1} cm^{-2} for lactate) and stability.

Sweat analysis. Sweat analysis is a non-invasive diagnostic method that provides information regarding the health of a human body. Sweat consists of vital biomarkers like glucose, lactate, urea, sodium, chlorine, calcium, potassium, protein, *etc.*, along with the primary component, water. These biomarkers can be analyzed to study the health of a person which is essential for medical diagnosis and athletic applications. Sweat is secreted by the sweat glands located below the skin. Hence, sweat sensors are generally placed directly on the skin as patches or tattoos. This requires the sensor to be biocompatible and skin conformal to yield good adhesion to the skin. Major challenges faced by sweat sensors are degradation after repeated usage, long response time, reduced shelf life, low sensitivity, and simultaneous measurement of multiple biomarkers. Lei *et al.* demonstrated a wearable sweat sensor using MXene for the first time to detect glucose, lactate, and pH (Fig. 9C–E).[49] The three-layered electrochemical sensor shown in Fig. 9A consists of (i) sweat uptake layer, which is adhering to the skin and is composed of serpentine tunnels and a porous fabric for sweat collection. When the sweat accumulates, sensors detect pH, glucose, and lactate levels. (ii) Sensing layer – for inserting active sensors consisting of sensor spaces and serpentine tunnels etched onto it. (iii) Cover layer – made of soft silicon rubber that introduces holes to allow oxygen diffusion towards the active sensor layer. This mold helps to protect from an open environment.

Thus, the excellent conductivity, 2D nature and solution processibility of MXenes pave the way for their integration with

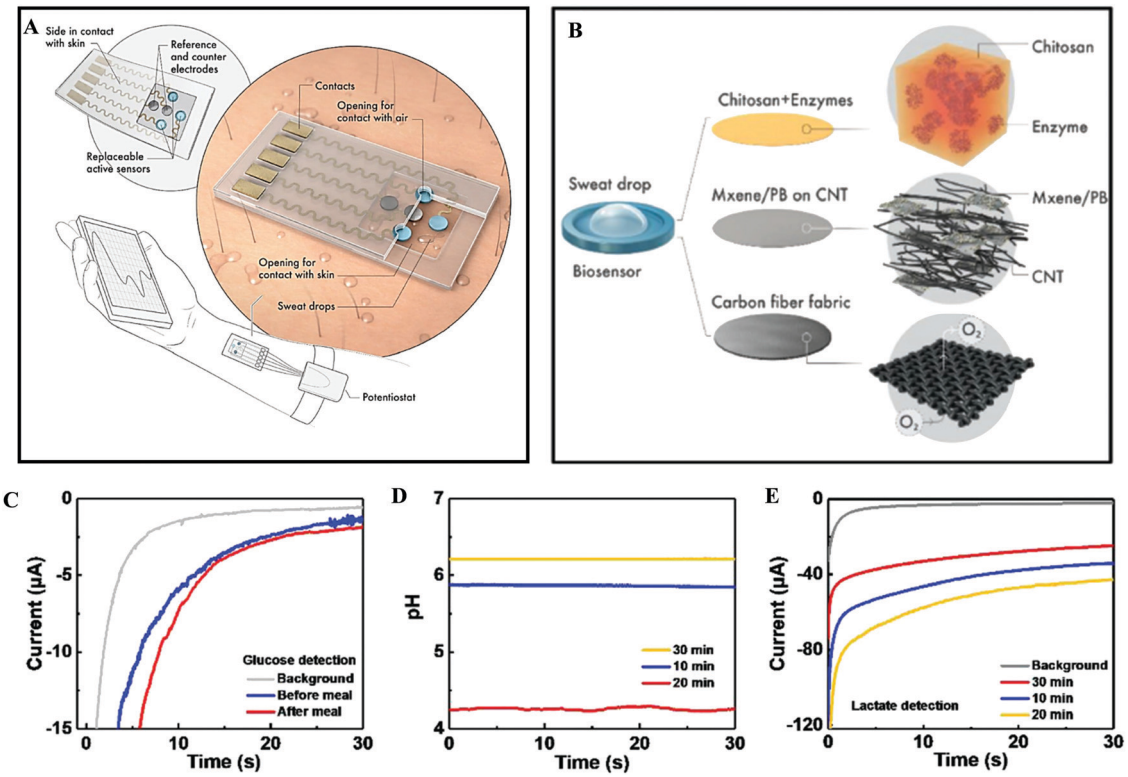

Fig. 9 Schematic illustrations of the bio-integrated sweat sensor. (A) Illustration of the system consisting of replaceable active sensors for collecting sweat droplets and driving them into a sealed serpentine tunnel. The pathway is pumped with a liquid metal alloy called Galinstan enabling high conductivity and mechanical stretchability. (B) The solid–liquid–air three-phase interface consists of CNT intercalated $Ti_3C_2T_x$/PB/CFMs (carbon fiber membranes) allowing oxygen to diffuse directly from the air phase at the bottom of the electrode to the respective enzyme. (C) Real-time body measurements carried out using the wearable patch indicating the glucose levels before and after intake of food, (D) pH levels taken at different time intervals during physical activity, and (E) chronoamperometric responses of the sensor to lactate levels measured at specific durations during the exercise. Reprinted with permission from ref. 49. Copyright John Wiley and Sons 2019.

the existing electrochemical system towards wearable sensing applications.

5.2.2 Gas sensors. Prevalent degradation of the air quality index in major cities and developing countries urges for the necessity of wearable gas sensors. Continuous and real-time monitoring of gases is vital for detection of hazardous and toxic gases in various environmental and industrial setups. While the exploration of gas sensors has been going on for years,[116] wearability is a recent attribute introduced that institutes several advantages in health monitoring and risk assessment applications. Wearability can be achieved by designing sensors that are flexible and biocompatible and at the same time have conserved the sensing characteristics. The key aspects of gas sensors are high sensitivity, low response time, a wide detection range over several gases and concentrations, high selectivity towards individual gases and the ability to detect gas molecules and chemical vapors at ultra-low concentrations. 2D materials have recently seen a lot of research interest in the development of gas sensors due to the exceptional properties they inherit. MXenes are currently one among the widely explored 2D materials for gas sensing applications. The layered structure of MXenes provides a large surface area for adsorption of gas molecules. The excellent metal-like conductivity aids better sensitivity and a high signal to noise ratio[117] as gas molecules induce a change in electrical response *via* physical and chemical adsorption. The abundant surface functional groups create strong binding to analyte molecules making them highly desirable candidates for gas sensing. MXene's versatile surface chemistry along with abundant adsorption sites is ideal for gas detection. The hydrophilicity and flexibility offered by this material also support adaptation for wearable applications. While several MXenes have been explored for gas sensing, the focus of this article was specifically on the use of $Ti_3C_2T_x$.

The key sensing mechanisms observed in MXene based gas sensors are surface charge transfer from the adsorbed gas molecules and Schottky barrier (SB) modulation. The adsorption of gas molecules on functionalized Ti_3C_2 surfaces and active defect sites result in change in the electrical resistance of the sensing film. This change in resistance is a function of majority charge carriers in the film and the electron donating/withdrawing behavior of the analytes. The gas sensitivity can be dramatically improved with the presence of the SB. For example, in a sensing material with electrons as mobility carriers, strong oxidizing gases can move the SB upward and resist the flow of electrons leading to a dramatic increase in gas sensitivity. Lee *et al.* reported the fabrication of Ti_3C_2 based wearable gas sensors on a flexible polyimide substrate for the sensing of volatile organic compounds (VOC).[117] The chemiresistive sensor was highly sensitive to exposure to an array of polar gases such as ethanol, methanol, acetone, and ammonia gas at room temperature. The Ti_3C_2sensor showed a p-type sensing behavior with highest and lowest response towards ammonia and acetone gas respectively. Lee *et al.* developed MXene/graphene hybrid fibers for NH_3 sensing.[118] A scalable wet spinning method was adopted to produce stable and flexible MXene/rGO fibers. These fibers which displayed excellent stability to mechanical deformations were woven into lab coats, illustrating their capability for wearable gas sensing applications. The flexible fiber geometry with a large surface to volume ratio showed 3 order higher sensitivity towards gas sensing compared to conventional rigid films. In a similar study, Zhao *et al.* reported a Ti_3C_2 MXene-cationic polyacrylamide (CPAM) nanocomposite for flexible NH_3 gas sensing.[119] These sensors displayed excellent selectivity towards ammonia, long term stability at room temperature and high flexibility for wearable applications. The addition of CPAM not only increased the mechanical stability of the rather fragile Ti_3C_2 MXene, but also the abundant surface functional groups of CPAM along with the formation of hydrogen bonding with the analyte gas dramatically improved the NH_3 sensitivity of the overall composite material. With several works reporting the capability of MXene and composite materials for sensing a variety of gases, their compatibility can be further investigated for wearable applications.

6. Outlook and prospects

MXenes are a new addition to the family of 2D materials with great potential in wearable sensing applications. The oxygen, hydroxyl, and fluorine terminations on their surface make MXenes hydrophilic and allow them to form stable water-based inks. The formation of surfactant-free colloidal solutions facilitates versatility in device fabrication, including various printing techniques. The rheological properties can be tuned to realize sensors *via* additive manufacturing. The ability of MXenes to form free-standing films enables design flexibility. Metallic conductivity along with hydrophilicity makes Ti_3C_2–MXene an excellent filler material to produce polymer composites. The piezoresistive property of MXene has been utilized in fabricating strain sensors useful for wearable sensing applications. The excellent material properties along with fabrication techniques were fine-tuned to design robust sensors for specific applications. Flexible wearable sensors have been fabricated that are ultrathin, lightweight, and durable with high sensitivity, a wide working range, and a fast response time. Wearable MXene strain sensors have drawn attention due to their flexibility, ultrasensitive range, and large stretchability. These sensors coupled to a wireless transmitter have futuristic applications towards real-time human motion detection, clinical diagnosis, and healthcare monitoring. In addition to that, multifunctional textiles could be endowed with highly sensitive humidity sensors while maintaining their flexible and porous features. Porosity and permeability also favours impressive electromagnetic intereference shielding efficiency that could have potential applications in military suits and gadgets.[120]

Despite these promising studies, the wearable applications of MXenes are still in the embryonic stage. The fabrication of flexible MXene devices has not been studied as extensively as that of graphene-based sensors. The issue with the stretchability of MXene nanosheets can be addressed by studying polymer composites with a wide range of biocompatible polymers.

The increased stretchability and wider sensing range will expand the scope of MXene devices for new applications. Different fabrication methodologies that include extrusion printing, 3D printing, and stamping can be utilized in the fabrication of wearable sensors on an industrial scale. From industrial aspect to environmental monitoring, MXene could be modified into gas sensors to detect volatile organic compounds with high sensitivity and low detection limit. They provide promising hybrids for gas sensing which could potentially be an additional feature in a wearable sensor. Wearable MXene sensors benefit a wide range of applications when all the features combined provide optimized results.

MXenes have also been used for the functionalization and immobilization of bioreceptors. They provide a platform for uniform and high-density binding of bioreceptors that enables fabrication of sensors for detection of analytes such as hemoglobin, glucose, lactate, cancer biomarkers, *etc.*[48,121] Compared to other 2D nanomaterials, MXenes have a unique set of properties (high conductivity, electrochemical activity, photothermal sensitivity, biocompatibility, immobilization of bioreceptors, and flexibility). These properties enable MXene to be used for wearable sensors that can detect both physical and physiological parameters directly from sweat. Recent review articles have comprehensively detailed the use of MXene based electrodes for electrochemical sensor applications.[122–125] While $Ti_3C_2T_x$–MXenes were utilized as a transducer material for detection of a wide range of biomarkers and analytes, the majority of the sensors reported were not body attachable systems. Thus, there is untapped potential to fabricate highly sensitive wearable electrochemical sensors. Interestingly, MXene was recently reported for urea removal,[126] where such properties prove to be useful for applications like enzyme-less urea detection in sweat. The reported work could potentially help in the early detection of kidney-related abnormalities and eventually aid in the tracking of other vital organs. Next, the self-reducing and catalytic properties of $Ti_3C_2T_x$–MXene provide the possibility to integrate MXenes with polymers/metals without hampering their activity to greatly improve sensor performance. Integration of electrochemical mediators with $Ti_3C_2T_x$–MXene sheets could help to reduce additional steps in the fabrication of self-sustainable wearable electrochemical sensors. Even for athletes, MXene electrochemical sensors could potentially detect the doping and stress level.

Next, surface functional groups are pivotal in determining various properties of MXenes as they can potentially modify conductivity, electrochemical activity, and plasmonic behavior. The selectivity of functional groups can tune the performance of wearable sensors and should be further investigated. The ability to modify the bandgap of MXenes is beneficial in exploring semiconducting properties and thus, showcasing possible applications in transistor-based devices. Furthermore, oxidation of MXene is a major issue that highly affects electrical conductivity and thus sensor performance. The ability to limit and control the amount of oxidation will provide stability to the sensor thereby increasing its shelf life. In this context, the stability of the sensors can be increased by providing additional encapsulation using hydrophobic and thermally insulated polymers.

Wearable sensors developed using MXene have immense prospects in diverse fields. Remote healthcare monitoring is critical for the elderly couple staying at home and for patients with chronic diseases. Wearable sensors provide a low-cost solution for continuous monitoring of health with major improvements in wearable experience. Inconspicuous user experience is essential for monitoring newborn babies. The practical application of wearable sensing involves dynamic measurements under the influence of various body parameters. The sensor response usually is a combination of multiple signals arising from different movements and temperature fluctuations. For example, the strain sensor attached to the wrist for real-time monitoring of artery pulse will also experience strain induced from the motion of the hand along with the blood pressure. Hence signal processing would play a vital role in procuring the essential data from the sensor output. However, a detailed analysis of sweat and muscle movements asks for the wearable system for prolonged engagement with physical activities of the human body. Therefore, the output of ultra-thin, flexible sensing elements needs to be amplified, filtered, modulated and communicated to the nearest smartphone for further processing and display. Consecutively merging polymer-based sensing elements with a flexible signal conditioning circuit will help bridge the technological gap between sensing, processing, and communication. Next, the signal conditioning module is generally a silicon integrated circuit embedded on a flexible circuit board that can be mounted on the skin easily. The circuit is then configured according to the need and type of signal. In addition to that, an RF or Bluetooth module can be attached for communication with the smartphone or the display unit. The advent of flexible batteries and antennas provides better alternatives to fabricate highly compact and flexible integrated circuits for wearable applications. Overall, such skin conformal modules increase the ergonomics of the entire system allowing real-time monitoring in complex applications, including infants. Further continuous and remote monitoring of a large group of people is required during the time of pandemic diseases where social distancing is necessary, especially during this COVID-19 crisis. Efforts are made to utilize wearable sensors integrated with IoT to constantly monitor people with likely symptoms of pandemic diseases.

Conflicts of interest

There are no conflicts to declare.

Acknowledgements

Saurabh Kumar is thankful to Prof. USN Murty, Director, National Institute of Pharmaceutical Education and Research (NIPER)-Guwahati for facilities. Financial support and facilities received from the Department of Science and Technology (DST/INSPIRE/04/2017/002750, INSPIRE Faculty award), New Delhi,

India and Centre for Nano Science and Engineering (CeNSE) at Indian Institute of Science (IISc), Bengaluru, India, respectively are sincerely acknowledged.

References

1 A. J. Bandodkar and J. Wang, Non-invasive wearable electrochemical sensors: a review, *Trends Biotechnol.*, 2014, **32**(7), 363–371.
2 S. C. Mukhopadhyay, Wearable sensors for human activity monitoring: a review, *IEEE Sens. J.*, 2014, **15**(3), 1321–1330.
3 J. T. Reeder, Y. Xue, D. Franklin, Y. Deng, J. Choi, O. Prado, R. Kim, C. Liu, J. Hanson and J. Ciraldo, Resettable skin interfaced microfluidic sweat collection devices with chemesthetic hydration feedback, *Nat. Commun.*, 2019, **10**(1), 1–12.
4 V. Shirhatti; S. Nuthalapati; V. Kedambaimoole; S. Kumar; M. M. Nayak and K. Rajanna, Laser-patterned multifunctional sensor array with graphene nanosheets as a smart biomonitoring fashion accessory. arXiv preprint, 2021, arXiv:2104.01615.
5 J. C. Yang, J. Mun, S. Y. Kwon, S. Park, Z. Bao and S. Park, Electronic Skin: Recent Progress and Future Prospects for Skin-Attachable Devices for Health Monitoring, Robotics, and Prosthetics, *Adv. Mater.*, 2019, **31**(48), 1904765.
6 X. Wang, L. Dong, H. Zhang, R. Yu, C. Pan and Z. L. Wang, Recent progress in electronic skin, *Adv. Sci.*, 2015, **2**(10), 1500169.
7 D.-H. Kim, N. Lu, R. Ma, Y.-S. Kim, R.-H. Kim, S. Wang, J. Wu, S. M. Won, H. Tao and A. Islam, Epidermal electronics, *Science*, 2011, **333**(6044), 838–843.
8 Z. Ma, D. Kong, L. Pan and Z. Bao, Skin-inspired electronics: emerging semiconductor devices and systems, *J. Semicond.*, 2020, **41**(4), 041601.
9 S. Kabiri Ameri, R. Ho, H. Jang, L. Tao, Y. Wang, L. Wang, D. M. Schnyer, D. Akinwande and N. Lu, Graphene electronic tattoo sensors, *ACS Nano*, 2017, **11**(8), 7634–7641.
10 C. Choi, Y. Lee, K. W. Cho, J. H. Koo and D.-H. Kim, Wearable and implantable soft bioelectronics using two-dimensional materials, *Acc. Chem. Res.*, 2018, **52**(1), 73–81.
11 A. J. Bandodkar, D. Molinnus, O. Mirza, T. Guinovart, J. R. Windmiller, G. Valdés-Ramírez, F. J. Andrade, M. J. Schöning and J. Wang, Epidermal tattoo potentiometric sodium sensors with wireless signal transduction for continuous non-invasive sweat monitoring, *Biosens. Bioelectron.*, 2014, **54**, 603–609.
12 H. L. Chia, C. C. Mayorga-Martinez, N. Antonatos, Z. K. Sofer, J. J. Gonzalez-Julian, R. D. Webster and M. Pumera, MXene Titanium Carbide-based Biosensor: Strong Dependence of Exfoliation Method on Performance, *Anal. Chem.*, 2020, **92**(3), 2452–2459.
13 B. Anasori, M. R. Lukatskaya and Y. Gogotsi, 2D metal carbides and nitrides (MXenes) for energy storage, *Nat. Rev. Mater.*, 2017, **2**(2), 1–17.
14 C. Ma, M. G. Ma, C. Si, X. X. Ji and P. Wan, Flexible Mxene-Based Composites for Wearable Devices, *Adv. Funct. Mater.*, 2021, **31**(22), 2009524.
15 M. M. Hasan, M. M. Hossain and H. K. Chowdhury, Two-dimensional MXene-based flexible nanostructures for functional nanodevices: a review, *J. Mater. Chem. A*, 2021, **9**(6), 3231–3269.
16 N. Li, J. Peng, W.-J. Ong, T. Ma, P. Zhang, J. Jiang, X. Yuan and C. J. Zhang, MXenes: an emerging platform for wearable electronics and looking beyond, *Matter*, 2021, **4**(2), 377–407.
17 K. Grabowski, S. Srivatsa, A. Vashisth, L. Mishnaevsky Jr and T. Uhl, Recent advances in MXene-based sensors for Structural Health Monitoring applications: a review, *Measurement*, 2021, 110575.
18 D. Lei, N. Liu, T. Su, L. Wang, J. Su, Z. Zhang and Y. Gao, Research progress of MXenes-based wearable pressure sensors, *Appl. Mater.*, 2020, **8**(11), 110702.
19 S. K. Bhardwaj, H. Singh, M. Khatri, K.-H. Kim and N. Bhardwaj, Advances in MXenes-based optical biosensors: a review, *Biosens. Bioelectron.*, 2022, 113995.
20 B. Zazoum, A. Bachri and J. Nayfeh, Functional 2D MXene Inks for Wearable Electronics, *Materials*, 2021, **14**(21), 6603.
21 H. Kim and H. N. Alshareef, MXetronics: MXene-Enabled Electronic and Photonic Devices, *ACS Mater. Lett.*, 2019, **2**(1), 55–70.
22 M. Ghidiu, M. R. Lukatskaya, M.-Q. Zhao, Y. Gogotsi and M. W. Barsoum, Conductive two-dimensional titanium carbide 'clay'with high volumetric capacitance, *Nature*, 2014, **516**(7529), 78–81.
23 J. Halim, S. Kota, M. R. Lukatskaya, M. Naguib, M. Q. Zhao, E. J. Moon, J. Pitock, J. Nanda, S. J. May and Y. Gogotsi, Synthesis and characterization of 2D molybdenum carbide (MXene), *Adv. Funct. Mater.*, 2016, **26**(18), 3118–3127.
24 P. Urbankowski, B. Anasori, K. Hantanasirisakul, L. Yang, L. Zhang, B. Haines, S. J. May, S. J. Billinge and Y. Gogotsi, 2D molybdenum and vanadium nitrides synthesized by ammoniation of 2D transition metal carbides (MXenes), *Nanoscale*, 2017, **9**(45), 17722–17730.
25 M. Ghidiu, M. Naguib, C. Shi, O. Mashtalir, L. Pan, B. Zhang, J. Yang, Y. Gogotsi, S. J. Billinge and M. W. Barsoum, Synthesis and characterization of two-dimensional Nb_4C_3 (MXene), *Chem. Commun.*, 2014, **50**(67), 9517–9520.
26 B. Anasori, C. Shi, E. J. Moon, Y. Xie, C. A. Voigt, P. R. Kent, S. J. May, S. J. Billinge, M. W. Barsoum and Y. Gogotsi, Control of electronic properties of 2D carbides (MXenes) by manipulating their transition metal layers, *Nanoscale Horiz.*, 2016, **1**(3), 227–234.
27 M. Naguib, O. Mashtalir, J. Carle, V. Presser, J. Lu, L. Hultman, Y. Gogotsi and M. W. Barsoum, Two-dimensional transition metal carbides, *ACS Nano*, 2012, **6**(2), 1322–1331.
28 O. Mashtalir, M. Naguib, V. N. Mochalin, Y. Dall'Agnese, M. Heon, M. W. Barsoum and Y. Gogotsi, Intercalation and delamination of layered carbides and carbonitrides, *Nat. Commun.*, 2013, **4**(1), 1–7.
29 J. Xuan, Z. Wang, Y. Chen, D. Liang, L. Cheng, X. Yang, Z. Liu, R. Ma, T. Sasaki and F. Geng, Organic-base-driven

intercalation and delamination for the production of functionalized titanium carbide nanosheets with superior photothermal therapeutic performance, *Angew. Chem.*, 2016, **128**(47), 14789–14794.

30 M. Alhabeb, K. Maleski, B. Anasori, P. Lelyukh, L. Clark, S. Sin and Y. Gogotsi, Guidelines for synthesis and processing of two-dimensional titanium carbide ($Ti_3C_2T_x$ MXene), *Chem. Mater.*, 2017, **29**(18), 7633–7644.

31 A. D. Dillon, M. J. Ghidiu, A. L. Krick, J. Griggs, S. J. May, Y. Gogotsi, M. W. Barsoum and A. T. Fafarman, Highly conductive optical quality solution-processed films of 2D titanium carbide, *Adv. Funct. Mater.*, 2016, **26**(23), 4162–4168.

32 M. Acerce, D. Voiry and M. Chhowalla, Metallic 1T phase MoS_2 nanosheets as supercapacitor electrode materials, *Nat. Nanotechnol.*, 2015, **10**(4), 313–318.

33 R. Raccichini, A. Varzi, S. Passerini and B. Scrosati, The role of graphene for electrochemical energy storage, *Nat. Mater.*, 2015, **14**(3), 271–279.

34 X. Wang, L. Zhi and K. Müllen, Transparent, conductive graphene electrodes for dye-sensitized solar cells, *Nano Lett.*, 2008, **8**(1), 323–327.

35 H. Chen, Y. Wen, Y. Qi, Q. Zhao, L. Qu and C. Li, Pristine Titanium Carbide MXene Films with Environmentally Stable Conductivity and Superior Mechanical Strength, *Adv. Funct. Mater.*, 2020, **30**(5), 1906996.

36 S. Hajian; P. Khakbaz; M. Moshayedi; D. Maddipatla; B. B. Narakathu; V. S. Turkani; B. J. Bazuin; M. Pourfath and M. Z. Atashbar in Impact of Different Ratios of Fluorine, Oxygen, and Hydroxyl Surface Terminations on Ti_3C_2Tx MXene as Ammonia Sensor: A First-Principles Study, *IEEE SENSORS*, IEEE, 2018, pp. 1–4.

37 D. L. Druffel, M. G. Lanetti, J. D. Sundberg, J. T. Pawlik, M. S. Stark, C. L. Donley, L. M. McRae, K. M. Scott and S. C. Warren, Synthesis and Electronic Structure of a 3D Crystalline Stack of MXene-Like Sheets, *Chem. Mater.*, 2019, **31**(23), 9788–9796.

38 C. Zhang, M. P. Kremer, A. Seral-Ascaso, S. H. Park, N. McEvoy, B. Anasori, Y. Gogotsi and V. Nicolosi, Stamping of flexible, coplanar micro-supercapacitors using MXene inks, *Adv. Funct. Mater.*, 2018, **28**(9), 1705506.

39 J. Liu, H. B. Zhang, R. Sun, Y. Liu, Z. Liu, A. Zhou and Z. Z. Yu, Hydrophobic, flexible, and lightweight MXene foams for high-performance electromagnetic-interference shielding, *Adv. Mater.*, 2017, **29**(38), 1702367.

40 Y. Z. Zhang, Y. Wang, Q. Jiang, J. K. El-Demellawi, H. Kim and H. N. Alshareef, MXene Printing and Patterned Coating for Device Applications, *Adv. Mater.*, 2020, **32**(21), 1908486.

41 T. Hu, M. Hu, Z. Li, H. Zhang, C. Zhang, J. Wang and X. Wang, Interlayer coupling in two-dimensional titanium carbide MXenes, *Phys. Chem. Chem. Phys.*, 2016, **18**(30), 20256–20260.

42 V. N. Borysiuk, V. N. Mochalin and Y. Gogotsi, Bending rigidity of two-dimensional titanium carbide (MXene) nanoribbons: a molecular dynamics study, *Comput. Mater. Sci.*, 2018, **143**, 418–424.

43 M. Kurtoglu, M. Naguib, Y. Gogotsi and M. W. Barsoum, First principles study of two-dimensional early transition metal carbides, *MRS Commun.*, 2012, **2**(4), 133–137.

44 A. Lipatov, H. Lu, M. Alhabeb, B. Anasori, A. Gruverman, Y. Gogotsi and A. Sinitskii, Elastic properties of 2D $Ti_3C_2T_x$ MXene monolayers and bilayers, *Sci. Adv.*, 2018, **4**(6), eaat0491.

45 X. Zhan, C. Si, J. Zhou and Z. Sun, MXene and MXene-based composites: synthesis, properties and environment-related applications, *Nanoscale Horiz.*, 2020, **5**, 235–258.

46 B. Anasori, M. R. Lukatskaya and Y. Gogotsi, 2D metal carbides and nitrides (MXenes) for energy storage, *Nat. Rev. Mater.*, 2017, **2**, 16098.

47 C. E. Ren, M. Q. Zhao, T. Makaryan, J. Halim, M. Boota, S. Kota, B. Anasori, M. W. Barsoum and Y. Gogotsi, Porous Two-Dimensional Transition Metal Carbide (MXene) Flakes for High-Performance Li-Ion Storage, *ChemElectroChem*, 2016, **3**(5), 689–693.

48 S. Kumar, Y. Lei, N. H. Alshareef, M. Quevedo-Lopez and K. N. Salama, Biofunctionalized two-dimensional Ti_3C_2 MXenes for ultrasensitive detection of cancer biomarker, *Biosens. Bioelectron.*, 2018, **121**, 243–249.

49 Y. Lei, W. Zhao, Y. Zhang, Q. Jiang, J. H. He, A. J. Baeumner, O. S. Wolfbeis, Z. L. Wang, K. N. Salama and H. N. Alshareef, A MXene-Based Wearable Biosensor System for High-Performance In Vitro Perspiration Analysis, *Small*, 2019, **15**(19), 1901190.

50 R. Rakhi, P. Nayak, C. Xia and H. N. Alshareef, Novel amperometric glucose biosensor based on MXene nanocomposite, *Sci. Rep.*, 2016, **6**, 36422.

51 K. Rasool, M. Helal, A. Ali, C. E. Ren, Y. Gogotsi and K. A. Mahmoud, Antibacterial activity of $Ti_3C_2T_x$ MXene, *ACS Nano*, 2016, **10**(3), 3674–3684.

52 H. Lin, Y. Chen and J. Shi, Insights into 2D MXenes for versatile biomedical applications: current advances and challenges ahead, *Adv. Sci.*, 2018, **5**(10), 1800518.

53 P. Cravedi, S. Farouk, A. Angeletti, L. Edgar, R. Tamburrini, J. Duisit, L. Perin and G. Orlando, Regenerative immunology: the immunological reaction to biomaterials, *Transplant Int.*, 2017, **30**(12), 1199–1208.

54 C. Dai, H. Lin, G. Xu, Z. Liu, R. Wu and Y. Chen, Biocompatible 2D titanium carbide (MXenes) composite nanosheets for pH-responsive MRI-guided tumor hyperthermia, *Chem. Mater.*, 2017, **29**(20), 8637–8652.

55 F. Wang, C. Yang, M. Duan, Y. Tang and J. Zhu, TiO_2 nanoparticle modified organ-like Ti_3C_2 MXene nanocomposite encapsulating hemoglobin for a mediator-free biosensor with excellent performances, *Biosens. Bioelectron.*, 2015, **74**, 1022–1028.

56 B. Akuzum, K. Maleski, B. Anasori, P. Lelyukh, N. J. Alvarez, E. C. Kumbur and Y. Gogotsi, Rheological characteristics of 2D titanium carbide (MXene) dispersions: a guide for processing MXenes, *ACS Nano*, 2018, **12**(3), 2685–2694.

57 Y. Yue, N. Liu, W. Liu, M. Li, Y. Ma, C. Luo, S. Wang, J. Rao, X. Hu and J. Su, 3D hybrid porous Mxene-sponge network

and its application in piezoresistive sensor, *Nano Energy*, 2018, **50**, 79–87.

58 Y. Guo, M. Zhong, Z. Fang, P. Wan and G. Yu, A wearable transient pressure sensor made with MXene nanosheets for sensitive broad-range human–machine interfacing, *Nano Lett.*, 2019, **19**(2), 1143–1150.

59 Y. Ma, N. Liu, L. Li, X. Hu, Z. Zou, J. Wang, S. Luo and Y. Gao, A highly flexible and sensitive piezoresistive sensor based on MXene with greatly changed interlayer distances, *Nat. Commun.*, 2017, **8**(1), 1207.

60 L. Yu, Z. Fan, Y. Shao, Z. Tian, J. Sun and Z. Liu, Versatile N-doped MXene ink for printed electrochemical energy storage application, *Adv. Energy Mater.*, 2019, **9**(34), 1901839.

61 J. Zhang, N. Kong, S. Uzun, A. Levitt, S. Seyedin, P. A. Lynch, S. Qin, M. Han, W. Yang and J. Liu, Scalable Manufacturing of Free-Standing, Strong $Ti_3C_2T_x$ MXene Films with Outstanding Conductivity, *Adv. Mater.*, 2020, 2001093.

62 M. Q. Zhao, C. E. Ren, Z. Ling, M. R. Lukatskaya, C. Zhang, K. L. Van Aken, M. W. Barsoum and Y. Gogotsi, Flexible MXene/carbon nanotube composite paper with high volumetric capacitance, *Adv. Mater.*, 2015, **27**(2), 339–345.

63 J. A. Rogers, Z. Bao, K. Baldwin, A. Dodabalapur, B. Crone, V. Raju, V. Kuck, H. Katz, K. Amundson and J. Ewing, like electronic displays: large-area rubber-stamped plastic sheets of electronics and microencapsulated electrophoretic inks, *Proc. Natl. Acad. Sci. U. S. A.*, 2001, **98**(9), 4835–4840.

64 B. N. Chandrashekar, A. S. Smitha, Y. Wu, N. Cai, Y. Li, Z. Huang, W. Wang, R. Shi, J. Wang and S. Liu, A universal stamping method of graphene transfer for conducting flexible and transparent polymers, *Sci. Rep.*, 2019, **9**(1), 1–11.

65 Y. Cai, J. Shen, G. Ge, Y. Zhang, W. Jin, W. Huang, J. Shao, J. Yang and X. Dong, Stretchable $Ti_3C_2T_x$ MXene/Carbon Nanotube Composite Based Strain Sensor with Ultrahigh Sensitivity and Tunable Sensing Range, *ACS Nano*, 2018, **12**(1), 56–62.

66 M. Singh, H. M. Haverinen, P. Dhagat and G. E. Jabbour, Inkjet printing—process and its applications, *Adv. Mater.*, 2010, **22**(6), 673–685.

67 A. Sridhar, T. Blaudeck and R. R. Baumann, Inkjet printing as a key enabling technology for printed electronics, *Mater. Matters*, 2011, **6**(1), 12–15.

68 S. Park, M. Vosguerichian and Z. Bao, A review of fabrication and applications of carbon nanotube film-based flexible electronics, *Nanoscale*, 2013, **5**(5), 1727–1752.

69 F. Torrisi, T. Hasan, W. Wu, Z. Sun, A. Lombardo, T. S. Kulmala, G.-W. Hsieh, S. Jung, F. Bonaccorso and P. J. Paul, Inkjet-printed graphene electronics, *ACS Nano*, 2012, **6**(4), 2992–3006.

70 C. J. Zhang, L. McKeon, M. P. Kremer, S.-H. Park, O. Ronan, A. Seral-Ascaso, S. Barwich, C. Ó. Coileáin, N. McEvoy and H. C. Nerl, Additive-free MXene inks and direct printing of micro-supercapacitors, *Nat. Commun.*, 2019, **10**(1), 1–9.

71 W. Yang, J. Yang, J. J. Byun, F. P. Moissinac, J. Xu, S. J. Haigh, M. Domingos, M. A. Bissett, R. A. Dryfe and S. Barg, 3D Printing of Freestanding MXene Architectures for Current-Collector-Free Supercapacitors, *Adv. Mater.*, 2019, **31**(37), 1902725.

72 I. Gibson; D. W. Rosen and B. Stucker, *Additive manufacturing technologies*. Springer, 2014, Vol. 17.

73 Z. Chen, Z. Li, J. Li, C. Liu, C. Lao, Y. Fu, C. Liu, Y. Li, P. Wang and Y. He, 3D printing of ceramics: a review, *J. Eur. Ceram. Soc.*, 2019, **39**(4), 661–687.

74 S. Sultan, H. N. Abdelhamid, X. Zou and A. P. Mathew, CelloMOF: nanocellulose enabled 3D printing of metal–organic frameworks, *Adv. Funct. Mater.*, 2019, **29**(2), 1805372.

75 F. Del Giudice and A. Q. Shen, Shear rheology of graphene oxide dispersions, *Curr. Opin. Chem. Eng.*, 2017, **16**, 23–30.

76 C. Bao, H. Zhang, C. A. Wilkie, S. Bi, X.-Z. Tang, J. Wu and J. Yang, On the dispersion systems of graphene-like two-dimensional materials: from fundamental laws to engineering guidelines, *Carbon*, 2016, **107**, 774–782.

77 E. García-Tuñón, E. Feilden, H. Zheng, E. D'Elia, A. Leong and E. Saiz, Graphene oxide: an all-in-one processing additive for 3D printing, *ACS Appl. Mater. Interfaces*, 2017, **9**(38), 32977–32989.

78 S. Roh, D. P. Parekh, B. Bharti, S. D. Stoyanov and O. D. Velev, 3D printing by multiphase silicone/water capillary inks, *Adv. Mater.*, 2017, **29**(30), 1701554.

79 J. Lewis, ADV FUNCT MATER, *Adv. Funct. Mater.*, 2006, **16**, 2193–2204.

80 J. Heikenfeld, A. Jajack, J. Rogers, P. Gutruf, L. Tian, T. Pan, R. Li, M. Khine, J. Kim and J. Wang, Wearable sensors: modalities, challenges, and prospects, *Lab Chip*, 2018, **18**(2), 217–248.

81 V. Kedambaimoole, N. Kumar, V. Shirhatti, S. Nuthalapati, S. Kumar, M. M. Nayak, P. Sen, D. Akinwande and K. Rajanna, Reduced Graphene Oxide Tattoo as Wearable Proximity Sensor, *Adv. Electron. Mater.*, 2021, **7**(4), 2001214.

82 V. Kedambaimoole, N. Kumar, V. Shirhatti, S. Nuthalapati, P. Sen, M. M. Nayak, K. Rajanna and S. Kumar, Laser-Induced Direct Patterning of Free standing Ti_3C_2–MXene Films for Skin Conformal Tattoo Sensors, *ACS Sens.*, 2020, **5**(7), 2086–2095.

83 Y. Gao, C. Yan, H. Huang, T. Yang, G. Tian, D. Xiong, N. Chen, X. Chu, S. Zhong and W. Deng, Microchannel-Confined MXene Based Flexible Piezoresistive Multifunctional Micro-Force Sensor, *Adv. Funct. Mater.*, 2020, **30**(11), 1909603.

84 Q. Yang, Z. Xu, B. Fang, T. Huang, S. Cai, H. Chen, Y. Liu, K. Gopalsamy, W. Gao and C. Gao, MXene/graphene hybrid fibers for high performance flexible supercapacitors, *J. Mater. Chem. A*, 2017, **5**(42), 22113–22119.

85 Z. Guo, N. Miao, J. Zhou, B. Sa and Z. Sun, Strain-mediated type-I/type-II transition in MXene/Blue phosphorene van der Waals heterostructures for flexible optical/electronic devices, *J. Mater. Chem. C*, 2017, **5**(4), 978–984.

86 Y.-Y. Peng, B. Akuzum, N. Kurra, M.-Q. Zhao, M. Alhabeb, B. Anasori, E. C. Kumbur, H. N. Alshareef, M.-D. Ger and

Y. Gogotsi, All-MXene (2D titanium carbide) solid-state microsupercapacitors for on-chip energy storage, *Energy Environ. Sci.*, 2016, **9**(9), 2847–2854.

87 T. Li, L. Chen, X. Yang, X. Chen, Z. Zhang, T. Zhao, X. Li and J. Zhang, A flexible pressure sensor based on an MXene–textile network structure, *J. Mater. Chem. C*, 2019, **7**(4), 1022–1027.

88 Z. Ling, C. E. Ren, M.-Q. Zhao, J. Yang, J. M. Giammarco, J. Qiu, M. W. Barsoum and Y. Gogotsi, Flexible and conductive MXene films and nanocomposites with high capacitance, *Proc. Natl. Acad. Sci. U. S. A.*, 2014, **111**(47), 16676–16681.

89 J. A. Rogers, T. Someya and Y. Huang, Materials and mechanics for stretchable electronics, *Science*, 2010, **327**(5973), 1603–1607.

90 W. H. Yeo, Y. S. Kim, J. Lee, A. Ameen, L. Shi, M. Li, S. Wang, R. Ma, S. H. Jin and Z. Kang, Multifunctional epidermal electronics printed directly onto the skin, *Adv. Mater.*, 2013, **25**(20), 2773–2778.

91 J.-H. Kim, S.-R. Kim, H.-J. Kil, Y.-C. Kim and J.-W. Park, Highly conformable, transparent electrodes for epidermal electronics, *Nano Lett.*, 2018, **18**(7), 4531–4540.

92 S. Wang, M. Li, J. Wu, D.-H. Kim, N. Lu, Y. Su, Z. Kang, Y. Huang and J. A. Rogers, Mechanics of epidermal electronics, *J. Appl. Mech.*, 2012, **79**(3), 031022.

93 T. Habib, X. Zhao, S. A. Shah, Y. Chen, W. Sun, H. An, J. L. Lutkenhaus, M. Radovic and M. J. Green, Oxidation stability of $Ti_3C_2T_x$ MXene nanosheets in solvents and composite films, *npj 2D Mater. Appl.*, 2019, **3**(1), 1–6.

94 C. J. Zhang, S. Pinilla, N. McEvoy, C. P. Cullen, B. Anasori, E. Long, S.-H. Park, A. S. Seral-Ascaso, A. Shmeliov and D. Krishnan, Oxidation stability of colloidal two-dimensional titanium carbides (MXenes), *Chem. Mater.*, 2017, **29**(11), 4848–4856.

95 J. Zhang, L. Wan, Y. Gao, X. Fang, T. Lu, L. Pan and F. Xuan, Highly stretchable and self-healable MXene/polyvinyl alcohol hydrogel electrode for wearable capacitive electronic skin, *Adv. Electron. Mater.*, 2019, **5**(7), 1900285.

96 V. Shirhatti, V. Kedambaimoole, S. Nuthalapati, N. Neella, M. Nayak and K. Rajanna, High-range noise immune supersensitive graphene-electrolyte capacitive strain sensor for biomedical applications, *Nanotechnology*, 2019, **30**(47), 475502.

97 T. Yang, X. Jiang, Y. Zhong, X. Zhao, S. Lin, J. Li, X. Li, J. Xu, Z. Li and H. Zhu, A wearable and highly sensitive graphene strain sensor for precise home-based pulse wave monitoring, *ACS Sens.*, 2017, **2**(7), 967–974.

98 H. Xu, J. Liu, J. Zhang, G. Zhou, N. Luo and N. Zhao, Flexible organic/inorganic hybrid near-infrared photoplethysmogram sensor for cardiovascular monitoring, *Adv. Mater.*, 2017, **29**(31), 1700975.

99 A. R. Maria; S. Pasca and R. Strungaru in Heart rate monitoring by using non-invasive wearable sensor, *E-Health and Bioengineering Conference (EHB)*, IEEE, 2017, pp. 587–590.

100 C. M. Boutry, L. Beker, Y. Kaizawa, C. Vassos, H. Tran, A. C. Hinckley, R. Pfattner, S. Niu, J. Li and J. Claverie, Biodegradable and flexible arterial-pulse sensor for the wireless monitoring of blood flow, *Nat. Biomed. Eng.*, 2019, **3**(1), 47–57.

101 A. Chhetry, J. Kim, H. Yoon and J. Y. Park, Ultrasensitive interfacial capacitive pressure sensor based on a randomly distributed microstructured iontronic film for wearable applications, *ACS Appl. Mater. Interfaces*, 2018, **11**(3), 3438–3449.

102 Y.-Z. Zhang, K. H. Lee, D. H. Anjum, R. Sougrat, Q. Jiang, H. Kim and H. N. Alshareef, MXenes stretch hydrogel sensor performance to new limits, *Sci. Adv.*, 2018, **4**(6), eaat0098.

103 Y. Ma, Y. Yue, H. Zhang, F. Cheng, W. Zhao, J. Rao, S. Luo, J. Wang, X. Jiang and Z. Liu, 3D synergistical MXene/reduced graphene oxide aerogel for a piezoresistive sensor, *ACS Nano*, 2018, **12**(4), 3209–3216.

104 X. Shi, H. Wang, X. Xie, Q. Xue, J. Zhang, S. Kang, C. Wang, J. Liang and Y. Chen, Bioinspired ultrasensitive and stretchable MXene-based strain sensor via nacre-mimetic microscale ''brick-and-mortar'' architecture, *ACS Nano*, 2018, **13**(1), 649–659.

105 S. Ryu, P. Lee, J. B. Chou, R. Xu, R. Zhao, A. J. Hart and S.-G. Kim, Extremely elastic wearable carbon nanotube fiber strain sensor for monitoring of human motion, *ACS Nano*, 2015, **9**(6), 5929–5936.

106 T. Yamada, Y. Hayamizu, Y. Yamamoto, Y. Yomogida, A. Izadi-Najafabadi, D. N. Futaba and K. Hata, A stretchable carbon nanotube strain sensor for human-motion detection, *Nat. Nanotechnol.*, 2011, **6**(5), 296.

107 J. Ren, C. Wang, X. Zhang, T. Carey, K. Chen, Y. Yin and F. Torrisi, Environmentally-friendly conductive cotton fabric as flexible strain sensor based on hot press reduced graphene oxide, *Carbon*, 2017, **111**, 622–630.

108 J. Shi, X. Li, H. Cheng, Z. Liu, L. Zhao, T. Yang, Z. Dai, Z. Cheng, E. Shi and L. Yang, Graphene reinforced carbon nanotube networks for wearable strain sensors, *Adv. Funct. Mater.*, 2016, **26**(13), 2078–2084.

109 J. Shi, J. Hu, Z. Dai, W. Zhao, P. Liu, L. Zhao, Y. Guo, T. Yang, L. Zou and K. Jiang, Graphene welded carbon nanotube crossbars for biaxial strain sensors, *Carbon*, 2017, **123**, 786–793.

110 S. Lim, D. Son, J. Kim, Y. B. Lee, J. K. Song, S. Choi, D. J. Lee, J. H. Kim, M. Lee and T. Hyeon, Transparent and stretchable interactive human machine interface based on patterned graphene heterostructures, *Adv. Funct. Mater.*, 2015, **25**(3), 375–383.

111 M. Liu, X. Pu, C. Jiang, T. Liu, X. Huang, L. Chen, C. Du, J. Sun, W. Hu and Z. L. Wang, Large-area all-textile pressure sensors for monitoring human motion and physiological signals, *Adv. Mater.*, 2017, **29**(41), 1703700.

112 J. J. Park, W. J. Hyun, S. C. Mun, Y. T. Park and O. O. Park, Highly stretchable and wearable graphene strain sensors with controllable sensitivity for human motion monitoring, *ACS Appl. Mater. Interfaces*, 2015, **7**(11), 6317–6324.

113 V. Kedambaimoole, N. Kumar, V. Shirhatti, S. Nuthalapati, M. M. Nayak and R. Konandur, Electric Spark Induced

Instantaneous and Selective Reduction of Graphene Oxide on Textile for Wearable Electronics, *ACS Appl. Mater. Interfaces*, 2020, **12**(13), 15527–15537.

114 A. N. De Loyola e Silva, A. Barfidokht, L. Yin, K. Y. Goud, M. A. Mohamed, E. Bailey and J. May, Epidermal enzymatic biosensors for sweat vitamin C: toward personalized nutrition, *ACS Sens.*, 2020, **5**(6), 1804–1813.

115 H. Teymourian, M. Parrilla, J. R. Sempionatto, N. F. Montiel, A. Barfidokht, R. Van Echelpoel, K. De Wael and J. Wang, Wearable electrochemical sensors for the monitoring and screening of drugs, *ACS Sens.*, 2020, **5**(9), 2679–2700.

116 A. Kaushik, R. Kumar, S. K. Arya, M. Nair, B. Malhotra and S. Bhansali, Organic–inorganic hybrid nanocomposite-based gas sensors for environmental monitoring, *Chem. Rev.*, 2015, **115**(11), 4571–4606.

117 E. Lee, A. VahidMohammadi, B. C. Prorok, Y. S. Yoon, M. Beidaghi and D.-J. Kim, Room temperature gas sensing of two-dimensional titanium carbide (MXene), *ACS Appl. Mater. Interfaces*, 2017, **9**(42), 37184–37190.

118 S. H. Lee, W. Eom, H. Shin, R. B. Ambade, J. H. Bang, H. W. Kim and T. H. Han, Room-temperature, highly durable $Ti_3C_2T_x$ MXene/graphene hybrid fibers for NH3 gas sensing, *ACS Appl. Mater. Interfaces*, 2020, **12**(9), 10434–10442.

119 L. Zhao, Y. Zheng, K. Wang, C. Lv, W. Wei, L. Wang and W. Han, Highly Stable Cross-Linked Cationic Polyacrylamide/$Ti_3C_2T_x$ MXene Nanocomposites for Flexible Ammonia-Recognition Devices, *Adv. Mater. Technol.*, 2020, **5**(7), 2000248.

120 L. X. Liu, W. Chen, H. B. Zhang, Q. W. Wang, F. Guan and Z. Z. Yu, Flexible and multifunctional silk textiles with biomimetic leaf-like MXene/silver nanowire nanostructures for electromagnetic interference shielding, humidity monitoring, and self-derived hydrophobicity, *Adv. Funct. Mater.*, 2019, **29**(44), 1905197.

121 P. K. Kalambate, N. S. Gadhari, X. Li, Z. Rao, S. T. Navale, Y. Shen, V. R. Patil and Y. Huang, Recent advances in MXene–based electrochemical sensors and biosensors, *TrAC, Trends Anal. Chem.*, 2019, 115643.

122 A. Sinha, H. Zhao, Y. Huang, X. Lu, J. Chen and R. Jain, MXene: an emerging material for sensing and biosensing, *TrAC, Trends Anal. Chem.*, 2018, **105**, 424–435.

123 P. K. Kalambate, N. S. Gadhari, X. Li, Z. Rao, S. T. Navale, Y. Shen, V. R. Patil and Y. Huang, Recent advances in MXene–based electrochemical sensors and biosensors, *TrAC, Trends Anal. Chem.*, 2019, **120**, 115643.

124 K. Deshmukh, T. Kovářík and S. K. Pasha, State of the art recent progress in two dimensional MXenes based gas sensors and biosensors: a comprehensive review, *Coord. Chem. Rev.*, 2020, **424**, 213514.

125 F. Shahzad, S. A. Zaidi and R. A. Naqvi, 2D Transition Metal Carbides (MXene) for Electrochemical Sensing: A Review, *Crit. Rev. Anal. Chem.*, 2020, 1–17.

126 F. Meng, M. Seredych, C. Chen, V. Gura, S. Mikhalovsky, S. Sandeman, G. Ingavle, T. Ozulumba, L. Miao and B. Anasori, MXene sorbents for removal of urea from dialysate: a step toward the wearable artificial kidney, *ACS Nano*, 2018, **12**(10), 10518–10528.